Thermodynamic and thermal comfort optimisation of a coastal social house considering the influence of the thermal breeze

Iván García Kerdan[a,b,*], David Morillón Gálvez[b], Gustavo Sousa[c], Santiago Suárez de la Fuente[d], Rodolfo Silva[b], Adam Hawkes[a]

[a] *Department of Chemical Engineering, Imperial College London, South Kensington Campus, London, SW7 2AZ, UK*
[b] *Instituto de Ingeniería, Universidad Nacional Autónoma de México, CDMX, México*
[c] *Sheffield School of Architecture, University of Sheffield, S10 2TN, UK*
[d] *Energy Institute, University College London, 14 Upper Woburn Pl, London, WC1H 0NN, UK*

Abstract

Tropical coastal areas are characterised by high levels of wind and solar resources with large potentials to be utilised for low-energy building design. This paper presents a multi-objective optimisation framework capable of evaluating cost-efficient and low-exergy coastal building designs considering the influence of the thermal breeze. An integrated dynamic simulation tool has been enhanced to consider the impacts of the sea-land breeze effect, aiming at potentiating natural cross-ventilation to improve occupant's thermal comfort and reduce cooling energy demand. Furthermore, the technological database considers a wide range of active and passive energy conservation measures. As a case study, a two-storey/two-flat detached social house located in the North-Pacific coast of Mexico has been investigated. The optimisation problem has considered the minimisation of: i. annual exergy consumption, ii. life cycle cost, and iii. thermal discomfort. Optimisation results have shown that adequate building orientation and window opening control to optimise the effects of the thermal breeze, combined with other passive and active strategies such as solar shading devices, an improved envelope's physical characteristics, and solar assisted air source heat pumps have provided the best performance under a limited budget. Compared to the baseline design, the closest to utopia design has increased thermal comfort by 93.8% and reduced exergy consumption by 10.3% whilst increasing the life cycle cost over the next 50 years by 18.5% (from US$39,864 to US$47,246). The importance of renewable generation incentives is further discussed as a counter effect measure for capital cost increase as well as unlocking currently high-cost low-exergy technologies.

Keywords: low-energy building, optimisation, solar design, exergy analysis, thermal breeze, thermal comfort

1. Introduction

Due to natural resource availability in coastal areas, the regional population and infrastructure are experiencing high growth rates, causing substantial socio-economic and environmental changes.

*Corresponding author
Email address: i.garcia-kerdan@imperial.ac.uk (Iván García Kerdan)

This has generated an increase in demand for affordable housing. On average, population densities in coastal cities are found to be three times higher compared to the world's average [1]. Currently, it is estimated that 23% of the world's population lives within 100 km distance of the coast and under 100 m above sea-level [2]. It is in these geographical locations where the sea-land breeze phenomena is mostly available.

In most developing economies, lack of appropiate building codes have caused housing designs to have poor energy and environmental performance [3]. However, most notorius have been the limited considerations for occupant's comfort which in turn has caused a wide range of health issues [4]. As income and population increases, the demand for comfort levels and healthier environments also increases [5]. Both, poor building designs and increase in household income could be considered as the main drivers for high growth rates in energy demand in the building sector [6]. This has been exacerbated in hot and humid climates, where poor designs have led to the widespread installation of oversized artifical air conditioners (AC), usually considered by practitioners as the only measure to provide occupants with comfortable thermal conditions. As a result, artificial space cooling is the fastest growing energy service in the building sector. Global energy demand from AC is expected to triple by 2050, contributing 21% of the total increase in final electricity demand [7]. Reducing future building energy use, especially cooling and heating demands, would play a fundamental role to achieve emissions targets and limit global warming to well below 2 °C [8].

To tackle poor energy performance of social housing and its dependency on high quality energy sources (electricity, natural gas), policies and regulatory shifts are necessary to improve cross-sectoral efficiency. Giannetti et al. [9] demonstrated the importance of using local resources in the development of sustainable social housing. A bioclimatic-oriented design and the utilisation of local available resources (local materials as well as solar and wind resources) should be encouraged at the early design stage, aiming at maximising the sustainability of the national social house stock. Smart architectural design, improved envelope characteristics, and efficient passive and active systems could be essential to reducing the impact of mechanical cooling in coastal social housing, allowing low-income families to improve indoor environmental quality (IEQ) and reduce energy bills.

McCabe et al. [10] provided a systematic review of the potential of using low-energy architectural designs and renewable-based technologies for social housing. The authors demostrated that the major historical barrier for its wider implementation has been the lack of appropriate tenant engagement and the over-complication of technological information. On the other hand, perceived economic benefits have the potential to act as the main motivational factor to installing renewable technologies in low-income houses. However, passive energy designs and optimal use of renewable energy technolgies in the coast is more difficult, especially when the building faces the opposite direction to solar energy. Usually, it is necessary to find design trade-offs between improved thermal and visual comfort as well as optimal solar energy harvesting throughout the year. For example, studies focusing on the advantages of incorporating bioclimatic strategies in coastal housing have demostrated that compared to active-oriented designs, optimal passive designs have improved IEQ and energy performance at lower capital and operational costs [11, 12]. On the contrary, Lebassi et al. [13] found that extensive installation of photovoltaic (PV) rooftops in coastal regions with hot climates have led to a positive thermal storage effect, increasing the Urban Heat Island (UHI)

effect by up to 0.2 °C.

1.1. The sea-land breeze effect and natural ventilation

Natural ventilation in buildings can be considered one of the most common bioclimatic strategies, with high energy efficiency potential in coastal buildings. Optimal utilisation of the thermal (sea-land) breeze can be found in vernacular architecture [11, 14], with limited incorporation in contemporary designs. However, in recent years, due to the expansion of offshore wind energy projects [15–17], knowledge on the onshore/offshore environment and coastal wind behaviour has substantially improved. Additionally, studies on wave energy resources [18], atmospheric research [19], air pollution transport and diffusion [20, 21] and island precipitation [22] have also contributed to the area. This has provided building energy researchers with a renewed awareness of understanding the thermal breeze behaviour, focusing on best ways of incorporating it into contemporary low-energy building designs [23].

Generally, the thermal breeze effect can be explained as follows: 1) during the day, land (which has a lower heat capacity than the sea) heats up quicker (heat island effect). As the air is heated up by conduction and rises due to its lower density, it starts to warm up the 'land's air' upper layers by convection. At the sea, as the amount of heat at surface level is much lower, the air is denser, and therefore, it does not rise. As the air over the land escapes the surface, it generates a pressure gradient (lower pressure is created), and at the sea, the lack of rising air creates higher surface pressure relative to the land. Thus, thermal circulation of warm air from the land towards the sea is generated. 2) To make up for the air that escaped from the land, the high pressure 'colder' air from the sea flows towards it. This is considered as the 'sea breeze' effect. At night, the opposite effect occurs. As land cools faster than sea due to their difference in heat capacities, cool air sinks over the land, while warm air rises over the sea, causing the air to flow from the land to the sea. This is considered as the 'land breeze' effect. Figure 1 illustrates the entire phenomenon.

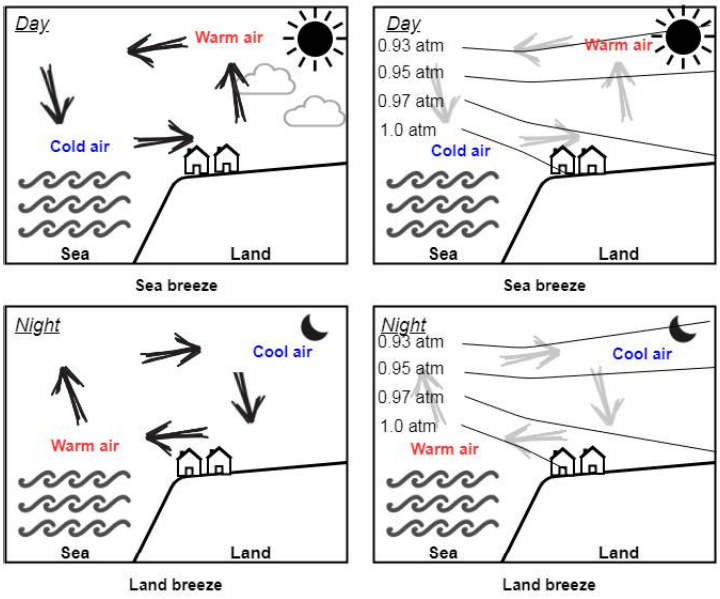

Figure 1: Sea-land breeze effect. On the left, the direction of the wind. On the right, atmospheric pressure at different altitudes (pressure decreases with increasing altitude)

In the built environment, an important research area that constantly studies the implications of thermal breezes is the UHI effect. UHI can cause micro-climate alterations [24], becoming a major concern for population's health and building energy use [25], especially in large dense cities [26]. Ichinose et al. [27] studied the interactions between the sea breeze and the UHI in Tokyo, Japan. In Tokyo, hot water infrastructure for commercial buildings is considered the largest contributor of anthropogenic heat. The authors found that the sea breeze variation throughout the year causes different heat fluxes rates, with a higher UHI effect during the winter, due to a weaker sea breeze from the Tokyo Bay combined with higher hot water demands from buildings.

The cooling effect that the sea-land breeze has on mitigating high temperatures and improving human thermal comfort has been demonstrated [28–31]. Recently, Xie et al. [32] studied the convective heat transfer rate on vertical surfaces in island-reef buildings. The optimal rate has been found at 21.5 W/m^2 K^{-1} under low-wind velocities, laying a solid foundation for the design of low-energy buildings in coastal areas. Locations close to large water bodies have the capacity to increase the cooling breeze effect. In coastal cities, many buildings, especially those located seaside, are designed with large windows facing the ocean to take advantage of the cooling sea breezes, avoiding heat storage during the day. At night, ventilation cools down the thermal mass, avoiding heat release during the day and therefore limiting over-utilisation of artificial cooling. Faggianelli et al. [33] investigated the use of thermal breezes to improve natural ventilation in houses located on the Mediterranean coast. To avoid complex modelling, the authors used a statistical wind rose supported by tracer gas measurements to investigate the implication of breezes in natural cross-ventilation flow rates. Outputs demonstrated that the best way of controlling air flow is by optimising building orientation and window opening angles, suggesting that minimal control on windows openings is necessary to maintain an airflow within comfortable conditions. However, the challenge is to detect optimal opening angles in real time, something that could be supported by building automation systems for ventilative cooling [34].

Bullen [35] investigated the design of coastal low-cost low-energy housing at a high wind speed location (Orkney Islands, Scotland). The main focus was to study the effects of sea breezes in cold climates. The author provided designs that minimise the exposure effects of high-wind and heavy-rain conditions while also considering building orientation, envelope thermal efficiency, solar gains, 'heating, ventilation and air conditioning' (HVAC) system efficiency, and draught-proofing. The final low-energy house design with improved thermal comfort conditions increased capital costs by 7.2% compared to a typical house in the region. Lebassi et al. [36] investigated how climatic variations in coastal California in the last thirty years have had an impact on degree-days and subsequently building energy demand. It was found that in coastal cities and near inland regions, cooling needs have asymmetrically increased in the last decades, reducing cooling degree-days (CDD) on the coast and increasing in inland regions. This has been mainly attributed to the sea breeze intensification, suggesting an increase in cold marine air, providing lower temperatures to coastal areas, thus reducing peak temperatures. Later, to understand this temperature asymmetry in the area, Lebassi et al. [13] investigated the environmental sustainability and thermodynamic implications of solar PV technologies, where large number of panels have been installed. Results showed that the large-scale presence of solar technologies have caused an increase in temperatures due to a net positive thermal storage effect. The authors discovered that this additional heat is being pushed inland as the sea breeze develops, warming further inland areas. Then, as the warmer

wind converges with the downwind from the hills, it produces additional hot spots inland. This effect have major implications for building adaptability, as current HVAC systems could become oversized/undersized, either increasing electricity demand or reducing ocupant's thermal comfort, especially in the hottest months [37].

However, the implications of the sea-land breeze at the coast also depends on other physical site conditions, such as location, terrain size, and particular surrounding characteristics [38]. For example, Rajagopalan et al. [39] examined the effect of the urban geometry of Muar, Malaysia on the city's wind flow. The unplanned development of the city (a combination of tall buildings with narrow streets) has reduced sea-land breeze air flows, increasing temperatures inside buildings at city level. A step-up configuration has been recommended to allow wind flows to reach deeper into the land. In this sense, computational fluid dynamics (CFD) and robust thermodynamic analysis are essential methods to gain a deeper understanding of the patterns and effects of thermal breezes.

1.2. Building thermodynamic analysis

Exergy is a concept that arises from the first law (energy conservation) and second law (entropy generation) of thermodynamics. According to Szargut [40], exergy can be defined as the amount of work obtainable when some matter is brought to a state of thermodynamic equilibrium with the common components of its surrounding nature by means of reversible processes. Exergy can be a useful tool in explaining sustainability of different energy sources and technologies [41]. Its implementation overcomes the limitations of the first law of thermodynamics by indicating locations, causes, and magnitudes of energy degradation (irreversibilities or exergy destructions), able to calculate meaningful efficiencies [42]. Consequently, exergy analysis is a method widely used for process systems and power plant design and optimisation [43]. In energy systems design, exergy analysis does not have to be seen as a replacement of typical energy analysis, but instead as a supplement, as a more efficient system can be achieved when exergy consumption and avoidable losses are minimised [44].

The majority of exergy related research that was dedicated to improving energy performance in an urban context has been applied to large scale systems, especially for district heating and neighbourhood-scale networks [45–47]. Nevertheless, exergy as a concept is becoming more popular among building energy researchers, and most importantly, among policy makers and practitioners [48, 49]. The studies from Shukuya [50] and Nieuwlaar and Dijk [51] describing the exergy-entropy process of building energy systems can be regarded as pioneers in the building energy research area. Shukuya's approach suggests that passive designs and not active systems are a prerequisite to realise exergy efficient systems. Other researchers, such as Meggers et al. [52], consider passive design too restrictive, suggesting that well-balanced designs between active and passive systems provide more design flexibility without compromising on exergy performance. Following, Meggers et al. [53] demonstrated that his hybrid approach provides better results in tropical climates by designing high-efficiency and high-temperature cooling systems. Also, thermal comfort has been studied using exergy. Assuming that thermal comfort is related to a minimum of exergy consumtion, Schweiker and Shukuya [54] compared an exergetic comfort model (human body exergy consumption (HBx-) rate) with the established adaptive comfort model and predicted mean vote (PMV) model, finding a linear relation between adaptive and exergetic model under neutral conditions. A review on the most recent building exergy literature can be found in Hepbasli [55] and

García Kerdan et al. [56].

The biggest limitation of using exergy analysis is concerning the selection of the reference temperature. The main difference with other research areas is that buildings' systems work very close (thermodynamically speaking) to the reference environment. Several authors have discussed whether static or dynamic temperatures provide more realistic outcomes. The IEA-Annex 49 [57], one of the most comprehensive research studies concerning exergy in buildings, suggest that a quasi-steady-state approach is suitable if storage systems are not considered. If the storage effect is considered then a dynamic analysis is necessary. Angelotti et al. [58] developed a dynamic method accounting for storage processes, requiring hourly temperature data for its assessment. The author compared the dynamic method against a steady-sate method by analysing a reversible air source heat pump (ASHP). It was concluded that although the dynamic method is more complex and time consuming, it provides a more comprehensive assessment, especially if cooling exergy is accounted for and the difference between internal and external temperature conditions are not greater than 10 K.

Choi et al. [59] presented a methodology for unsteady-state exergy analysis deriving energy, entropy and exergy governing equations to tackle transient heat conduction problems. The authors verified the method against steady-state and transient processes, providing exegetic behaviour that is not possible to capture with steady-state analysis. On the other hand, Pons [60] argues that a time-dependent dynamic reference environment might not be suitable as it could be biased to the fluctuations in ambient temperatures. Therefore, he suggests a static dead-state reference temperature to reduce uncertainties, demonstrating its applicability for both cooling and heating exergy demand. Li et al. [61], proposed to examine exergy flows based on "cool" and "warm" exergy using heat pumps as case study. This method allows to differentiate between exergy sources, tracking them throughout the whole building energy supply chain, identifying what type of systems are able to extract cool exergy from the environment. Similarly, Kazanci et al. [62], analysed the exergy performance of different space cooling systems by separating "cool" and warm" exergy in the analysis, enabling designers to appropriately quantify the exergy content of a heat source or a sink. Nevertheless, more evidence is still required among the building research community in order to reach an agreement on the most appropriate reference temperature.

1.3. Building design optimisation

Optimisation has been a popular approach in building research in the last years [63, 64]. The most popular objectives to be optimised have been energy demand, capital and operational costs, carbon emissions, and occupant's thermal comfort [63]. Stochastic methods based on genetic algorithms (GA) can be regarded as the most utilised method for building energy optimisation [64]. Recent optimisation studies have focused on the application of artifical neural networks for tool performance improvement [65] and novel mixed integer linear frameworks [66, 67]. In terms of technologies, recent studies have focused on the integration of renewable energy [68, 69] and thermal properties optimisation of state-of-the-art phase change materials (PCM) [70]. Most recently, Chen and Yang [71], by using a surrogate-based optimisation model and considering the improvement of energy performance and thermal comfort, investigated the influence of climate conditions on passively designed buildings, exploring optimal designs at different climates in mainland China.

The combination of exergy analysis and multi-objective optimisation studies applied to a combined passive and active building design has been rather limited. García Kerdan et al. [72], focusing on renovation projects, presented an optimisation framework considering the minimisation of exergy consumption throughout the entire building energy supply chain, exploring a wide range of active and passive measures in a commercial building located in a cold climate. Later, the framework was improved by including economic and exergoeconomic analyses [73]. Similarly, Di Somma et al. [74] applied an exergy-based multi-objective optimisation of distributed energy systems aiming at reducing project's costs and improving exergy efficiency by considering energy qualities of different supply sources. Gas-fired combined heat and power (CHP) systems were found among the most efficient systems to reduce primary exergy input, while solar technologies provided the best exergetic performance due to the availability of free renewable exergy.

Still, more research is necessary that considers the implications and interactions of distinct active and passive systems in buildings, aiming at improving thermodynamic performance, reducing costs and increasing occupant's thermal comfort, especially in locations where climatic conditions are most favourable due to the availability of renewable energy resources such as solar and wind.

1.4. Research gaps

After a thorough search of the relevant literature, it was found that there is limited thermodynamic-oriented modelling frameworks that appropriately consider the effects of local bioclimatic conditions, and especially the thermal breeze effect in coastal regions, for the optimal design of low-energy/exergy and cost-efficient buildings. Additionally, existing tools lack relevant databases which consider a wide range of passive and active technologies with robust techno-economic characterisation that could be applied indistinctly to any building and region. Therefore, the aim of this study is threefold. First, to include the dynamic effect of the thermal breeze in a recently developed exergy-based dynamic simulation tool. The tool provides EnergyPlus [75] with the capability of performing dynamic exergy calculations, thanks to an external Python-based subroutine. Secondly, to built a comprehensive database considering different passive and active technologies within the context of coastal regions. And thirdly, to demonstrate the model's capabilities, a social house located in the Mexican North-Pacific coast is studied and optimised under different thermodynamic and economic objectives.

The paper is organized as follows. First, an overview of the optimisation framework, the selected wind energy and exergy methods and the description of building technologies are presented. Later, the case study and the optimisation problem formulation are given. Next, the paper presents the obtained results from the optimisation procedure, followed by a design comparison between a selected optimal design (obtained from the Pareto front) with the benchmark design. This is followed by discussions and finally conclusions arising from this study.

2. Methodology and case study

2.1. ExRET-Opt: a dynamic exergy analysis optimisation tool

ExRET-Opt [73], is a novel building energy/exergy optimisation open-source tool developed by the authors. It is based on EnergyPlus [75] for dynamic energy simulations, combined with Python-based [76] routines for dynamic exergy analysis and exergoeconomic accounting. The

model's second law analysis module is capable of calculating thermodynamic indices such as exergy consumption, exergy efficiencies and exergoeconomic parameters throughout the entire energy supply chain providing a more comprehensive analysis for the researcher or building designer. The exergetic analysis is mainly based on the work from the ECB-Annex 49 methodology [57], while the exergoeocnomic analysis is based on the SPECO method developed by Lazzaretto and Tsatsaronis [77]. Both methods were further improved and adapted for whole building energy systems in García Kerdan et al. [78]. An overview of the main exergy calculation method can be found in Appendix A.

An additional strength of the tool is the large techno-economic database of passive and active energy technologies that incorporates, allowing the exploration of a wide range of design combinations (>4 quadrillion different combinations). In this study, several technology options have been added (Section 2.3). As the search space can be too large to perform full-parametric studies, to reduce simulation times, the tool is capable to simulate a limited number of solutions by using different sampling methods (Monte Carlo, Morris method, and Latin Hypercube). Additionally, a multi-objective optimisation mode based on genetic algorithms (NSGA-II) is available to improve designs in time-constraint studies.

2.2. Thermal breeze wind analysis

The main focus of this study has been to understand the potential of the thermal breeze in the design of a low-exergy building, as such, this section illustrates the derived model integrated into the dynamic exergy calculation tool.

As the sea-land breeze effect is a three-dimensional and dynamic effect throughout the day, dynamic simulations are required to fully account for its impact in the building's physics. EnergyPlus is able to calculate the thermal effect of wind for each exposed surface, necessary to account for exterior convection, as it alters infiltration and ventilation flows throughout the analysed thermal zones. Therefore, appropriate data on wind speed and direction are required to produce the climatological file (.epw file), which is an important input to the model. However, this kind of data is limited, as normally data at a given location and specific height is available. When this is the case, EnergyPlus calculates wind speeds at different altitudes by means of extrapolation using the following equation:

$$v_z = v_{met}(\frac{\delta_{met}}{z_{met}})^{\alpha_{met}}(\frac{z}{\delta})^{\alpha} \tag{1}$$

where z is the altitude height above ground [m], v_z is the wind speed at altitude z [m s^{-1}], α is the wind speed profile exponent at the site [-], δ is the wind speed profile boundary layer thickness at the site [-], while z_{met}, V_{met}, α_{met} and δ_{met} is the height above ground [m], wind speed measured [m s^{-1}], wind speed profile exponent [-], and wind speed profile boundary layer thickness [m] respectively at the meteorological station. As wind parameters depend on the surroundings (type of terrain and nearby constructions), for the specific case of coastal areas, α is assumed as 0.10 and δ as 100 m.

With the complete wind profile, the ventilation flow rate given by the thermal breeze throughout the entire building envelope can be calculated as follows [79]:

$$Q_w = C_w A_{opening} F_{schedule} V \tag{2}$$

where Q_w is the volumetric air flow rate driven by the breeze [m3 s^{-1}], C_w is the opening effectiveness [-], $A_{opening}$ is the opening area [m2], $F_{schedule}$ is the open area fraction [-] and V is the local wind speed [m s^{-1}]. In EnergyPlus, these equations can be accesed by using the object: `ZoneVentilation:WindandStackOpenArea` and the Thermal Analysis Research Program (TARP) convection model algorithm [75].

Then, it is necessary to calculate hourly building energy demand considering the effects of natural ventilation ($q_{dem,vent,i}(t_k)$). Commonly, due to temperature differences between the outside and the inside environments, energy flows would escape or enter the building through the envelope via transmission and ventilation. Using Eq. 3, the internal load can be calculated as follows [79]:

$$q_{dem,vent,i}(t_k) = \rho C_p Q_w \Delta T(t_k) \tag{3}$$

where ρ is the the outdoor air density [kg m^{-3}], C_p is the specific heat coefficient [1.007 kJ $kg^{-1}K^{-1}$], A is the thermal area [m] of zone i, and ΔT the differential between the outdoor temperature ($T(t_k)$) and the indoor temperature ($T_0(t_k)$) [K].

Finally, to obtain the exergy demand considering the ventilation flow due to the thermal breeze effect, the following formula based on the Carnot factor can be used:

$$Ex_{dem,vent,zone}(t_k) = \sum_{i=1}^{n} \left(q_{dem,vent,i}(t_k) * \left(1 - \frac{T_0(t_k)}{T_i(t_k) - T_0(t_k)} ln \frac{T_i(t_k)}{T_0(t_k)} \right) \right) \tag{4}$$

where, T_i is the average inside temperature [K], $q_{dem,vent}$ is the energy demand due to ventilation [kWh], t_k is the time-step [-], and n is the number of analysed thermal zones. As typical convention, heating energy is regarded as positive ($q+$) while cooling energy as negative (q-), defining the direction of the energy flow. However, as defined by Shukuya [80] and the ECB-Annex49 [57] method, the exergy flow would depend not only the heat flow direction, but also on the indoor and ambient temperatures. In the case of space cooling, when the required internal temperature is higher than the outside temperature (mainly due to high internal heat gains), it means that there is exergy available indoors that needs to be extracted, thus an exergy output is required (Ex-). On the other hand, when the required indoor temperature needs to be lower than the outside, an exergy input is required bringing cool exergy indoors ($Ex+$). In order to keep the indoor temperature at a comfortable range, it is required to supply cool exergy at a rate higher than the cool exergy escaping from the building.

This group of equations form the basis for the calculation of minimum amount of work (thermal exergy) necessary to cover thermal demands in buildings with high natural ventilation rates. Eq. 4 has been added to ExRET-Opt enabling the quantification of exergy demand considering both internal gains and ventilation effects due to thermal breezes.

2.3. Design strategies

The technological database has been expanded by including several solar passive and active strategies as well as other energy efficiency measures. Table 1 presents the techno-economic data for all possible energy efficiency measures available in this study.

Table 1: Techno-economic database of possible active and passive measures

Passive measures			
Type	**Technology/measure**	**Description**	**Cost unitary/range**
Glazing	*Single pane*	5mm clear pane	133 US$ m^{-2}
	Double-pane	5mm clear pane with 6 or 13mm gap filled with either air, argon or krypton	349-494 US$ m^{-2}
	Triple-pane	5mm clear pane with 6 or 13mm gap filled with either air, argon or krypton	624-873 US$ m^{-2}
Insulation	*Polyurethane*	2 to 15 in 1 cm steps	8.87-31.01 US$ m^{-2}
	Extruded polystyrene (XPS)	1 to 15 in 1 cm steps	6.34-42.54 US$ m^{-2}
	Expanded polystyrene (EPS)	2 to 15 in 1 cm steps	5.78-13.23 US$ m^{-2}
	Cellular Glass	4 to 18 in 1 cm steps	21.55-97.01 US$ m^{-2}
	Glass Fibre	6.7 7.5 8.5 and 10 cm	7.51-10.3 US$ m^{-2}
	Cork board	2 to 30 in 2 cm steps	7.40-114.11 US$ m^{-2}
	Phenolic foam board	2 to 10 in 1 cm steps	7.42-29.11 US$ m^{-2}
	Aerogel	0.5 to 4 in 0.5 cm steps	35.64-259.53 US$ m^{-2}
	PCM (w/board)	10 and 20 mm	76.8-143.3 US$ m^{-2}
Solar protection	*Overhangs*	Material: PVC module with 20 mm width	39.9 US$ m^{-2}
	Fins	Length: 0.05 to 2.0 m	
Active measures			
Type	**Technology/measure**	**Description**	**Unitary cost**
HVAC system	*Air source heat pumps*	COP: 2.5	601.6 US$ kW^{-1}
	Ground source heat pumps	COP: 3.5 (horizontal boreholes)	1596 US$ kW^{-1}
	District cooling + HX + radiant cooling	Trigeneration: single-effect indirect-fired CHP with absorption chiller with a COP of 0.7.	75 US$ kW^{-1} district heat exchanger 6140 US$ connection charge and 66.5 US$ m^{-1} insulation for pipes
Cooling emission system	*Variable Air Volume (VAV) (GSHP and ASHP only)*	Single duct VAV with cooling efficiency of 72.2% and auxiliary energy demand of 14.82 W m^{-2}	931 US$ per system
Lighting	*CFL lamps*	Low wattage lamps with low ballast factor. Power density: 10.7 W m^{-2}	153 US$ kW^{-1}
	LED	Low wattage solid-state lamps. Power density : 3.7 W m^{-2}	295 US$ kW^{-1}
Active solar renewable	*Solar PV*	Monocrystalline silicon panels with module efficiency of 13-15%	852 US$ m^{-2}
	Solar collectors	Flat plate solar thermal collector (HSTC) with efficiency between 60-80%. 40% propylene glycol/water mixture and pump efficiency of 87%	382 US$ m^{-2}
Other renewable	*Wind turbines*	Small scale wind turbines (micro) 1.0 - 1.5 kW	1000-3000 US$ per unit
Control	*Window automatic control*	Chain actuators with PID control	150 US$ per window plus home control system

Most of the passive strategies aim at optimising heat flows by improving building's envelope physical characteristics. Constructive strategies such as the usage of an air gap in the composite walls as a means to reduce insulation thickness has been considered. Additionally, a window control system for opening at certain angles are simulated to allow for effective cross-ventilation and/or night flush cooling; while solar shading are considered as low-cost measures to minimise solar gains. For active solar systems, collectors and photovoltaic panels have been considered.

2.4. Case study: The Mexican coastal region

In 2015, the Mexican residential sector was responsible for 14.8 % (755 PJ) of the national energy demand [81], emitting around 21,280 Gg CO_2eq [82]. It was estimated that coastal housing was responsible for over 30% of these emissions [82]. Mexico's coast extends over more than 11,000 km and it is considered one of the largest and most dynamic commercial areas, and key for the development of the country's economy [83]. Around 15% of the population live in coastal areas and are currently expierencing higher population growth rates than inland cities [84]. Added to this, a constant increment in household income and demand increase for thermal comfort have led to a rise in the installation and energy demand of artificial cooling. According to McNeil et al. [85], 35% of households located in hot climates own an air conditioner (AC), with an average cooling capacity of 5.3 kW per household. By 2050, AC ownership is expected to reach 50%, while household cooling capacity to increase to 6.3 kW. Just emissions related to additional cooling demand could reach about 10,000 Gg CO^2eq by 2030. Therefore, new strategies and programmes are necessary to limit these emissions without compromising the health and life quality of the population.

To test the proposed optimisation framework, a social house in the city of 'Cabo San Lucas, Baja California Sur (BCS)', located in the Mexican North-Pacific coast has been selected as a case study (Figure 2). The city has a population of 85,000 inhabitants, with annual growth rates of about 3.8%, well above the national average of 1.3%. Generally, the BCS state is located in the arid climatic region; however, the southern region, where Cabo San Lucas is located, is considered tropical, lying just under the Tropic of Cancer. The climate throughout the year is mostly hot and humid, with daily average temperatures just over 30 °C during the summer. The region posses one of the highest solar irradiation potentials in the country, with levels above 5.8 kW m^{-2} (Figure 2).

To justify the presence of artificial air conditioners in a social house in the region, according to government's official figures [86], there is a probability of 32.3% that a social house in Cabos, BCS would have an air conditioning. For the lowest income groups living in social housing, the probability is as low as 15.4%, while for the highest income the probability is as high as 93.4%. The report also suggest that 46% of the total installed equipment are 'window' type while 54% are mini-splits.

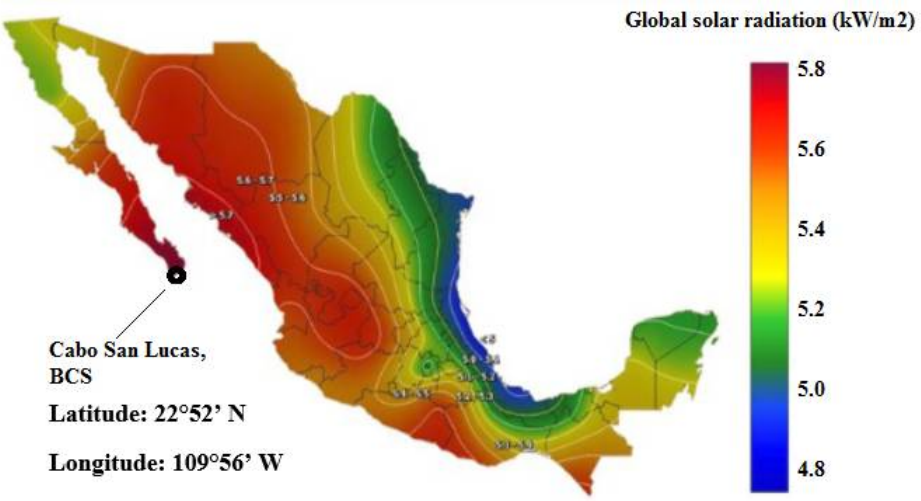

Figure 2: Annual average incident solar radiation in Mexico: Modified from: CONUEE [87]

For the climatological file, hourly data such as air temperature, relative humidity, atmospheric pressure, and radiation parameters have been collected from Meteonorm [88]. Additionally, data on wind speeds and wind directions from regional thermal breezes have also been collected. Figure 3 illustrates the distribution of wind direction and wind velocities for the city. It can be seen that most of the winds come from the south and west directions, with average air velocities of about 3.5 m s^{-1}; however, wind speeds over 5 m s^{-1} are frequent.

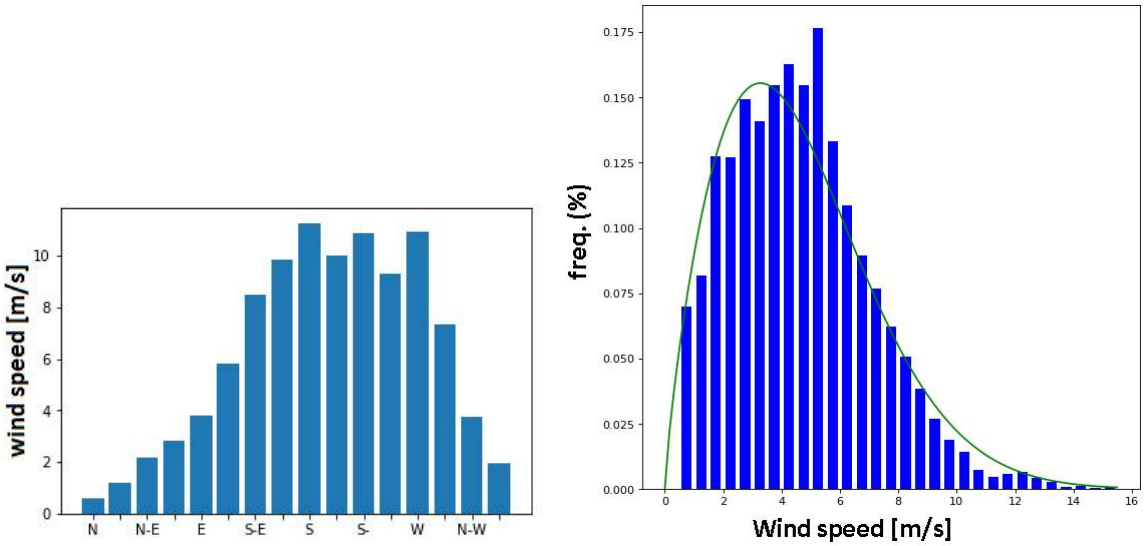

Figure 3: Wind direction and wind speed distribution (with fitted Weibull density function) for Cabo San Lucas, Mexico

To better appreciate the wind direction and speed in relation to the case study's geography, a wind rose summarising the wind profile and the coast location is shown in Figure 4. As expected, the majority of the sea breeze, characterised by stronger winds, comes from the South and South-West, while land breezes are most predominant from the West and North-West regions. One of

the main advantages of thermal breezes is that directions remain fairly constant through the year, which provides an easier assessment for the development of optimal building orientation to improve cross-ventilation strategies.

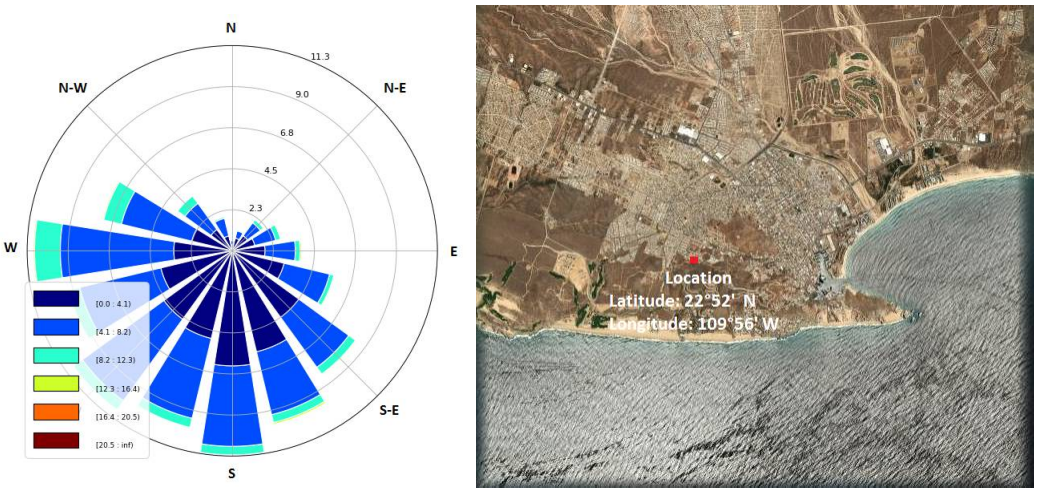

Figure 4: Wind Rose (left) and location for Cabo San Lucas, Mexico (wind data: velocity in m s^{-1} and frequency; Map source: Microsoft Bing Maps [89])

A two-storey/two-flat house has been chosen. This layout represents FOVISSSTE's (the state's housing fund) 'duplex D' archetype social house design. Detailed information can be found in the supplementary data (S.1). On average, social house under the defined category (duplex D) is about 51 m^2, while for the case study is around 62 m^2 . Each flat is comprised of two bedrooms, a living-dining room, a kitchenette and a bathroom. Also, solar shading is considered in the base design as a low-cost measure. The 3D model is illustrated in Figure 5.

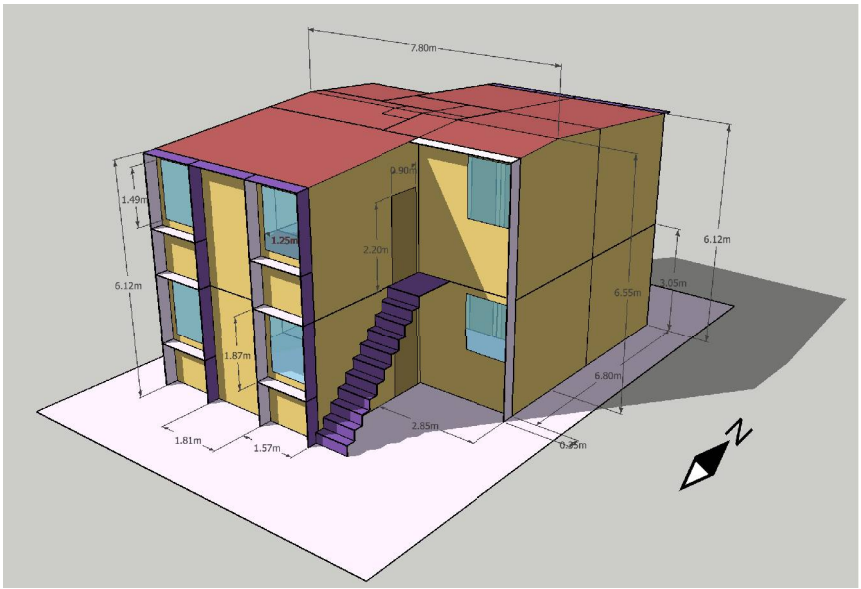

Figure 5: Typical two storey/two flat social house layout in Mexico's hot climates

2.5. Baseline thermal performance: Calibration

The baseline building energy performance has been calibrated based on electricity demand values obtained from several regional studies [90, 91]. As a pre-processing step, the ExRET-Opt optimisation mode has been used to reduce the difference between the model's monthly energy use and the empirilcal data. This optimisation approach minimises the Coefficient of Variation of the Root Mean Squared Error (CVRMSE) [92].

$$min[CVMRSE(\%)] = \frac{\sqrt{\frac{\sum_{i=1}^{N_p}(m_i - s_i)^2}{N_p}}}{\bar{m}} \tag{5}$$

where m_i is the empirical value for month i, s_i is the predicted value for month i, N_p is the sample size (N=12), and $\bar{m}$ is the mean value of the empirical data ($\sum_{i=1}^{N_p}(m_i/N_p)$). When monthly data is used, a CVRMSE up to 0.15 is tolerable to consider a model calibrated.

For the calibration process, based on the current Mexican energy regulations [93], constrains on building physical characteristics (mainly envelope's U_{values}) and energy systems efficiency have been considered. Table 2 shows the main building design parameters and thermodynamic values obtained. The calibrated baseline building has a total energy use index (EUI) of 268.1 (kWh $m^{-2}y^{-1}$). Electricity represents 76% of the total energy use, while the rest is covered by liquefied petroleum gas (LPG). Cooling demand represents 46.5% of the total supplied electricity, followed by electric appliances (35.3%) and lighting (16.0%). The simulation process also estimated the cooling equipment installed capacity (4.9 kW for the bottom flat and 5.6 kW for the top flat), converging with those values presented in McNeil et al. [85] ($\sim$ 5 kW). On the other hand, LPG is mainly used for water heating (51%) and cooking (49%). Annual energy bills have been found just above US$ 1,100 per flat. The model has considered a price of 0.063 US$ kWh^{-1} for electricity and 0.052 US$ kWh^{-1} for LPG. Accounting for the whole energy supply chain, the building consumed exergy in the order of 513.6 kWh $m^{-2}y^{-1}$, with an exergetic efficiency (ψ) of 11.3%. This value is found within range, compared to those found in other studies in similar climates (ψ = 9.0-12.1%) [94].

Table 2: Calibrated baseline model main characteristics

Baseline characteristics	**Social housing (North-west Mexico)**
Year of construction	2018
Number of floors/flats	2/2
Total floor space (m^2)	130 (65 m^2 per flat)
Orientation (°)	East-West (180° with respect to the north)
Infiltration rate (ach)	4.0
Exterior Walls	Cavity Wall-Brick walls 130 mm brick with 20mm air gap + external insulation (50 mm expanded polystyrene) U_{value} = 0.45 (W $m^{-2}K^{-1}$)
Roof	160 mm concrete block + external insulation (130 mm expanded polystyrene) U_{value} = 0.26 W $m^{-2}K^{-1}$
Ground floor	100 mm concrete slab U_{value} = 0.52 W $m^{-2}K^{-1}$
Windows	Single-pane clear glass (5mm thick) U_{value} =5.84 W $m^{-2}K^{-1}$
Glazing ratio	7%
HVAC System	Window air conditioning system 4.9 kW bottom flat, 5.6 kW top flat $\eta = 90\%$ No heating system
Emission system	Fan system and natural ventilation
Cooling Set Point (°C)	22.5
Occupancy (people)	3-4 per flat
Equipment (W m^{-2})	3.9
Lighting level (W m^{-2})	10.7
$EUI_{electricity}$ (kWh $m^{-2}y^{-1}$)	211.3
EUI_{LPG} (kWh $m^{-2}y^{-1}$)	66.8
Annual energy bill (US$ y^{-1})	1,105 per flat
Thermal discomfort (hours)	1,460
CO_2 emissions (energy) (Ton)	8.2 per flat
Life cycle cost - 50 years (US$)	39,865
Total annual exergy input (kWh $m^{-2}y^{-1}$)	579.2
Annual exergy consumption (kWh $m^{-2}y^{-1}$)	513.6
Building exergy efficiency (%)	ψ = 11.3

2.6. Optimisation problem

The optimisation problem has been designed to simultaneously optimise the following three objectives:

i. Building annual exergy consumption ($Ex_{cons,bui}$ [kWh m^2 y^{-1}]):

$$Z_1(x)min = Ex_{cons,bui} = \left[\sum_{f=1}^{f} Ex_{prim}(t_k) - \sum_{i=1}^{i} Ex_{dem,enduse,i}\right] \quad (6)$$

where Ex_{prim} is the sum of primary exergy input from fuel f (f= electricity, gas, lpg) and $\mathrm{Ex}_{dem,enduse,i}$ is the exergy demand at end use service i (i= cooling, dhw, appliances, cooking).

ii. Occupant discomfort hours (based on the Predicted Mean Vote Index (PMV) expressed by the Fanger's model [95]):

$$Z_2(x)min = (|PMV| > 0.5) = |(0.303e^{-0.036M} + 0.028)L| > 0.5 \quad (7)$$

where M is the metabolic rate [W m^{-2}], L is the thermal load defined by the difference between the internal heat gains of occupancy per unit area and the heat loss to the environment [W m^{-2}], and e is the Euler's number [$e = 2.718$]. The index was primarily developed to assess the impacts of mechanically ventilated buildings in thermal comfort; thus, careful assessment needs to be made for natural ventilated (NV) buildings as PMV values could be over or under predicted.

iii. Life Cycle Cost - 50 years (US$):

$$Z_3(x)min = LCC_{50years} = \sum_{n=1}^{N}\left[\frac{CF_n}{(1+r_d)^n}\right] \quad (8)$$

where CF_n is the annual cash flow of year n [US$ y^{-1}], N is the total years of evaluation, and r_d is the discount rate [%]. The annual cash flow can be calculated as follows:

$$CF_n = \left[(C_n^B + O\&M_n^B) + (C_n + O\&M_n) + (C_{en})\right] \quad (9)$$

where C_n^B is the baseline capital cost [US$], $O\&M_n^B$ is the baseline operation and maintenance cost [US$], C_n is the incremental capital cost in year n [US$], $O\&M_n$ is the incremental operation and maintenance cost in year n [US$], and C_{en} is the annual energy cost [US$].

Therefore, the optimisation model can be formulated as follows.

$$\text{Given} \quad x = \left\langle X^{glaz}, X^{wall,ins}, X^{roof,ins}, X^{shade}, X^{HVAC}, X^{setpoint}, X^{light}, X^{PV}, X^{wind}, X^{col}\right\rangle$$

in the solution space X, find the vector(s) x that:

$$\text{minimises} \quad Z(x^*) = Z_1(x*), Z_2(x*), Z_3(x*)$$

The model has been constrained considering the following maximum costs and discomfort time values:

s.t:

$$\begin{cases} \text{LCC(x)} \leq \text{US\$ 90,000} \\ \text{Discomfort(x)} \leq 10\% \text{ occupied time} \end{cases}$$

Table 3 shows the NSGA-II algorithm settings defined in the model. The NSGA-II procedure embedded within the ExRET-Opt tool is further explained in the Appendix B.

Table 3: NSGA-II algorithm parameters and stopping criteria for optimisation with GA

Parameters	
Encoding scheme	Integer encoding (discretisation)
Population type	Double-Vector
Population size	50
Crossover Rate	100%
Mutation Rate	40%
Selection process	Stochastic fitness influenced
Tournament Selection	2
Elitism size	Pareto optimal solutions
Stopping criteria	
Max Generations	100
Time limit (s)	10^6
Fitness limit	10^{-6}

3. Results and discussion

3.1. Constrained solutions and adopted measures

Following the optimisation run, 4,800 distinct designs have been collected. Different to other optimisation approaches, solutions with high output heterogeneity can be found due to the gene crossover, mutation and selection processes. In this study, 25% of the solutions were found in the constrained region. Figure 6 illustrates the final solutions as well as the Pareto front.

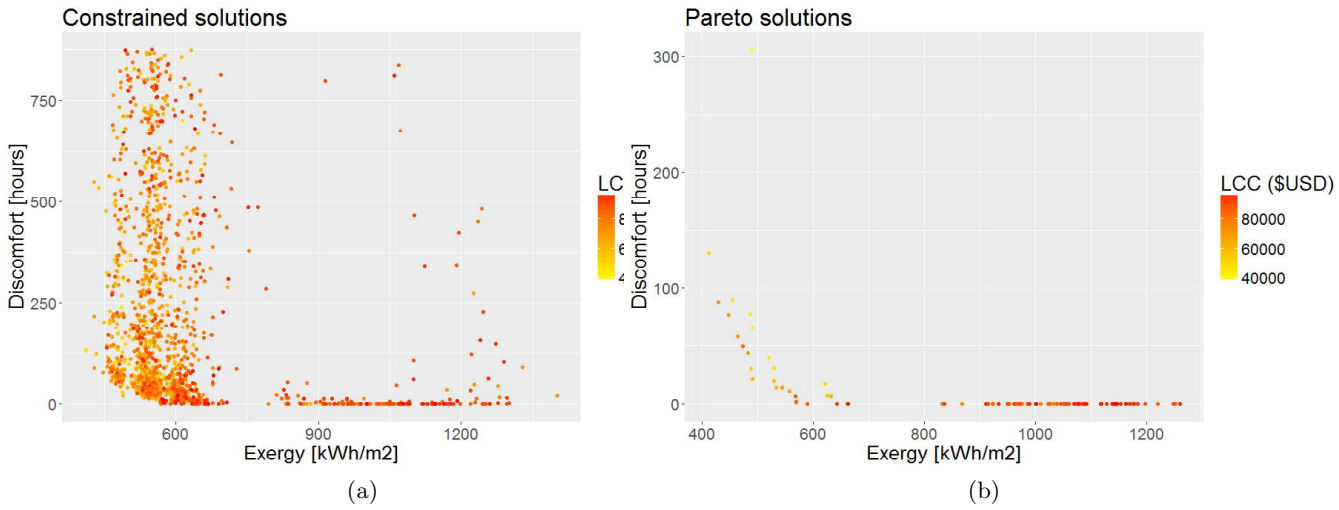

Figure 6: Optimisation results found in a) the constrained region and, b) the Pareto front

Generally, higher cost designs have provided the best comfort levels; however, at the expense of higher energy use and exergy consumption due to the more intensive utilisation of artificial cooling equipment, with average temperature set-points of around 23 °C. Additionally, these designs are mainly based on high insulation levels, triple-pane windows and oversized active solar technologies (collectors and PV panels), which in turn have increased capital expenditure.

Figure 7 illustrates the distributions of the most important active and passive design strategies found in the constrained region (see the Nomenclature section for labels). As shown, among the most popular adopted passive measures have been double-pane glazing (either filled with air, argon or krypton), expanded polyestyrene (EPS) and cellular glass with thickness between 2 and 12 cm for both wall and roof insulation, as well as solar shading devices (Appendix C, Figure C.1). The most common values for overhangs has been found at 0.95 m, while for right and left fins at 1.15 and 0.80 m respectively; however, optimal lengths for solar shading greatly depends on building's solar gains and orientation. In this regard, the most common orientations have been found between 170-190° (east-west orientation considering the North as reference at 0°). Within this orientation range, the thermal breeze impacts the building's main façade directly as the most frequent and strongest winds come from the south (sea breeze). When windows on both sides are open, this maximises cross-ventilation flow rates. During the day and with low wind speeds this provides comfort levels to the occupants; however, higher wind speeds (around 3 m s^{-1}), which are frequent in the analysed region, could produce discomfort. This could be addressed by controlling the window's opening angles [33]. Among the most widely adopted active systems, solar PV panels covering between 10-30% of the roof area, 10-20 m^2 of solar collectors, LED lighting and ASHPs have been found.

The most frequent rejected measures, due to cost or performance issues, have been high surface areas of PV panels (> 60% roof area) and solar collectors (>40 m^2). Also, GSHPs and district cooling have not been as widely adopted as ASHPs, mainly due to high capital costs. However, designs based on GSHPs typically provided the lowest exergy consumption, while district cooling networks combined with wall emission systems provided the best solutions for thermal comfort.

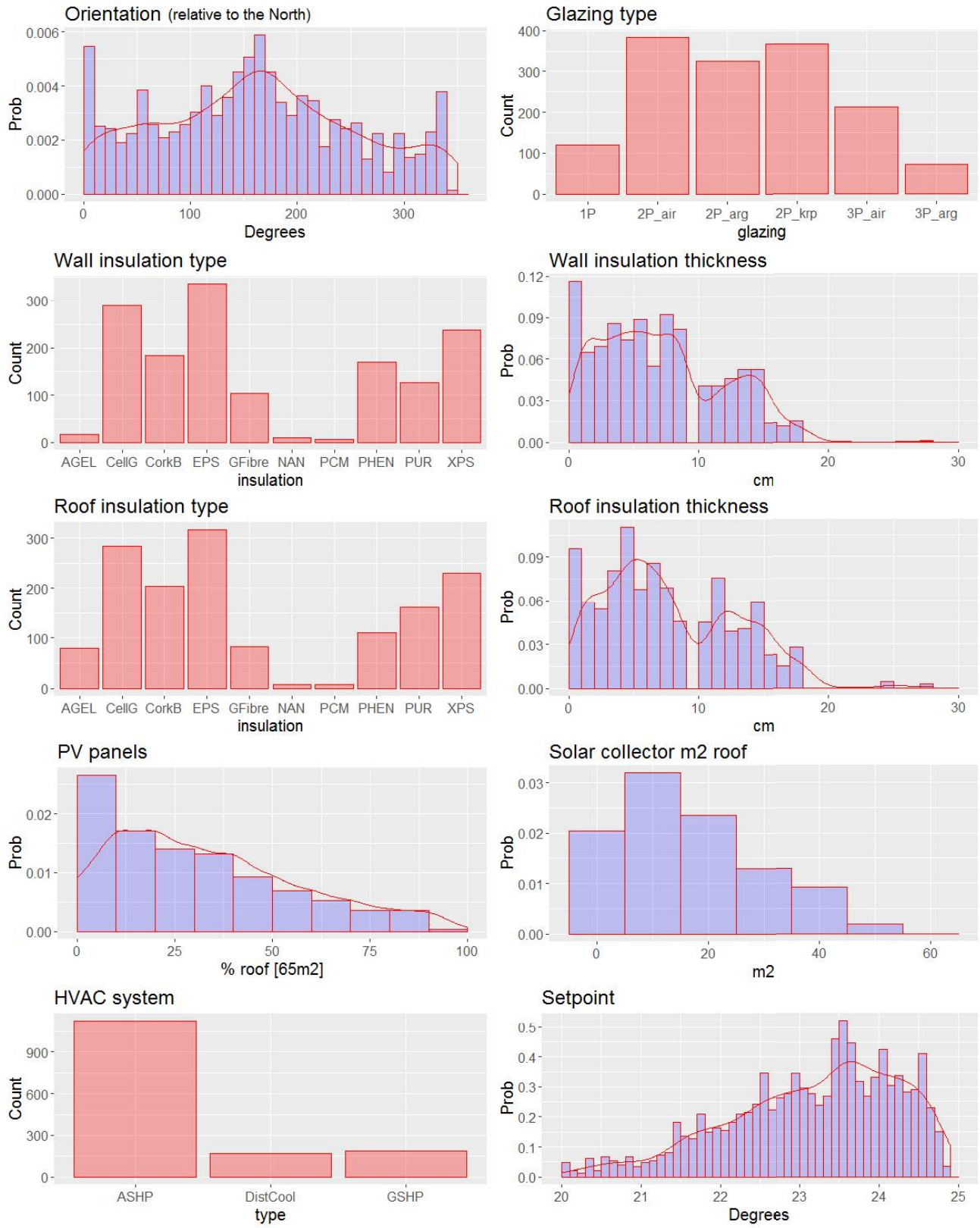

Figure 7: Distribution (bars) and the fitted probability distribution (lines) of main design parameters for the constrained solutions

Among the analysed objective functions, the average values for exergy consumption, discomfort hours and LCC have been found at 617 kWh $m^{-2}y^{-1}$, 219 hours, and US$ 74,387 respectively. Compared to the baseline values, exergy consumption and LCC have increased due to dramatic improvements in thermal comfort. However, these designs count with a larger share of renewable generation (mainly from solar technologies) and low-exergy cooling equipment (such as heat pumps), which have increased capital costs considerably. As the exergy analysis method used in this model does not make a distinction between exergy use from fossil fuels or renewable energy, irreversibilities in the system using either grid electricity or from PV generation are regarded similarly. If renewable exergy use were not to be considered, the average consumption would be reduced to 522 kWh $m^{-2}y^{-1}$, similar to the baseline value. An important parameter that has been greatly improved thanks to on-site generation was the annual energy bill, as average values were found at US$ 703 per flat, representing savings in the order of 36.4%. This reduction has been achieved without considering the effect of feed-in tariffs or incentives from renewable generation, as these programmes are not yet implemented in the country. Otherwise, this would help minimise project's life cycle cost and increase the return of investment, possibly unlocking other more expensive low-exergy technologies such as ground source heat pumps and/or high temperature district cooling systems.

3.2. Pareto front solutions and adopted measures

Figure 8 illustrates the design parameters distribution exclusively from the Pareto front (n= 109) (Figure 6b). In these 'optimal' solutions, the most common measures have been the following: reduced area for PV panels (10% of roof area, equivalent to about 1.1 kWp), large solar collectors areas (up to 40 m2, or 60% of the roof area), connection to a district cooling network, double-pane air filled glazing, 5 cm (range: 1-10 cm) of extruded polyesthyrene (XPS) for wall insulation, 9 cm (range: 1-15 cm) of polyurethane for roof insulation, and an orientation of 45° or 225° with respect to the north axis.

With regards to the building orientation, the most common Pareto values (45° and 225°) represent a further improvement compared to the mean value found in the constrained solution (170-190°). This affirmation is based on the study from Givoni [96], where the author recommended that angles between 30° and 60° relative to the main breeze axis allows for better pressure control and ventilation flow. However, he also mentioned that ventilation from thermal breezes will either reduce cooling requirements or improve thermal comfort, but not both. Therefore, the outputs from our Pareto front illustrate that optimal solutions preferred to use natural cross-ventilation and specific active and passive strategies for thermal comfort improvement (an increase of 99.2% compared to the baseline, reducing annual discomfort hours to 11 hours), while average exergy consumption were found at 915 kWh (an increase of 80.5%). High irreversibilities arise due to higher utilisation of the cooling equipment at night, as heat gains during day-time ventilation were being released by the building's thermal mass at night. Night ventilation, which is the opposite strategy, could have been followed as it can cool the building mass and store cold to be utilised during the day; however, this strategy is optimised when the building has high insulation levels, an air-tight envelope, and closed windows throughout the day. This strategy deprives the design to take advantage of the day-time thermal breezes for thermal comfort.

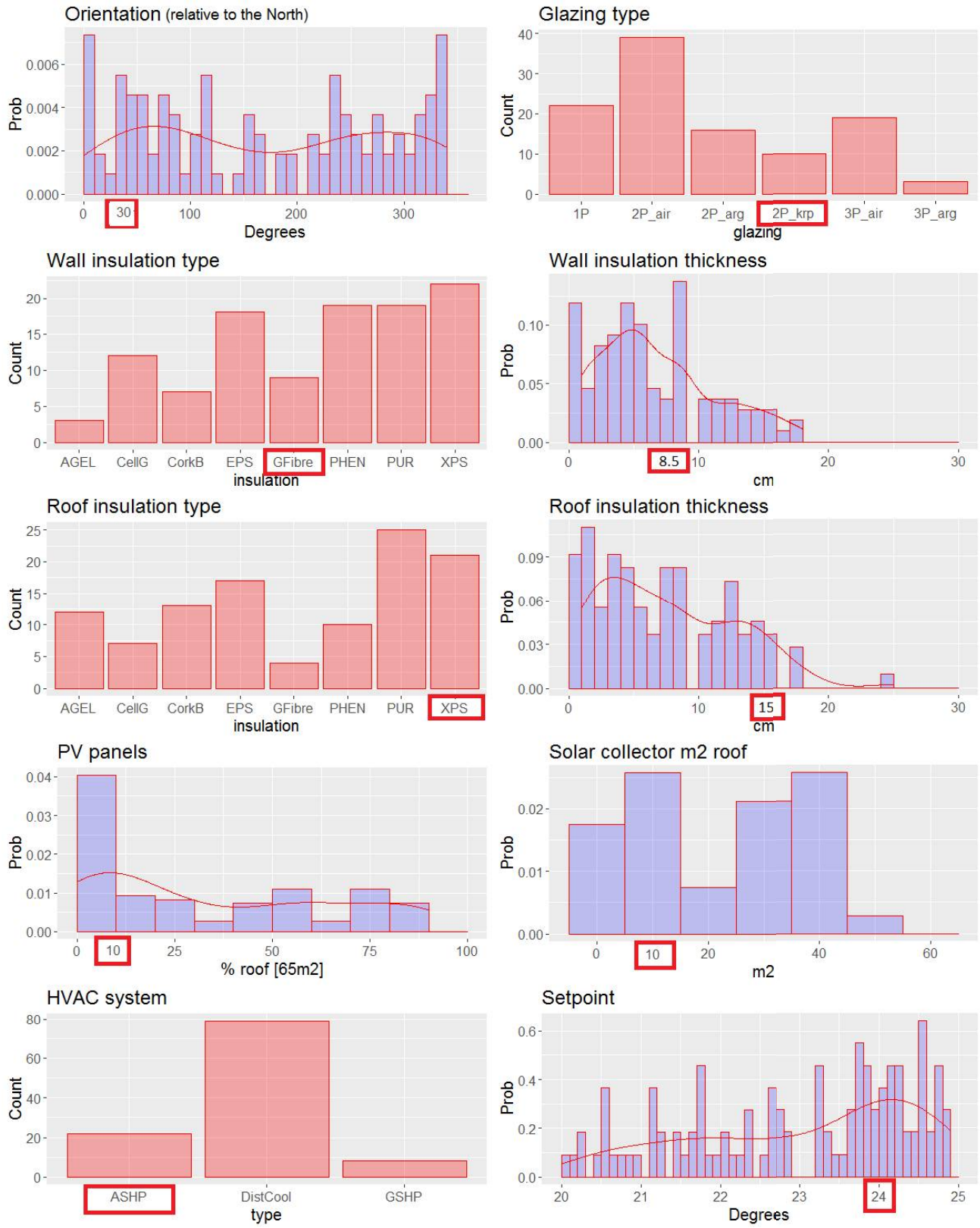

Figure 8: Distribution (bars) and the fitted probability distribution (lines) of main design parameters for the Pareto front highlighting the 'closest to utopia' (CTU) design

The Pareto designs have also come with a two-fold increase in life cycle cost, reaching an average value of US$ 82,413. At this point, it can be concluded that the optimisation procedure instead of converging on designs that utilised the sea-land breeze effect for high thermodynamic and low-cost performance, it was converging on designs where the the thermal breeze (mainly sea breeze at day-time) was exploited for the improvement of thermal comfort. Also, when analysing the objetive's convergence (Figure 9), thermal comfort converged to its minimum value from the 2^{nd} generation, while exergy consumption and life cycle cost did it at the 78^{th} and 59^{th} generation respectively. Therefore, most of the designs resulted in solutions with high cost, high exergy use and high thermal comfort due to what can be called an 'algorithm failure'. This takes place when at some point in the evolution process, the optimisation process between generations finds it difficult to move and find other more balanced solutions. The discussed designs that shift the objective function mean outputs, can be seen by the Pareto's right 'tail' illustrated in Figure 6b.

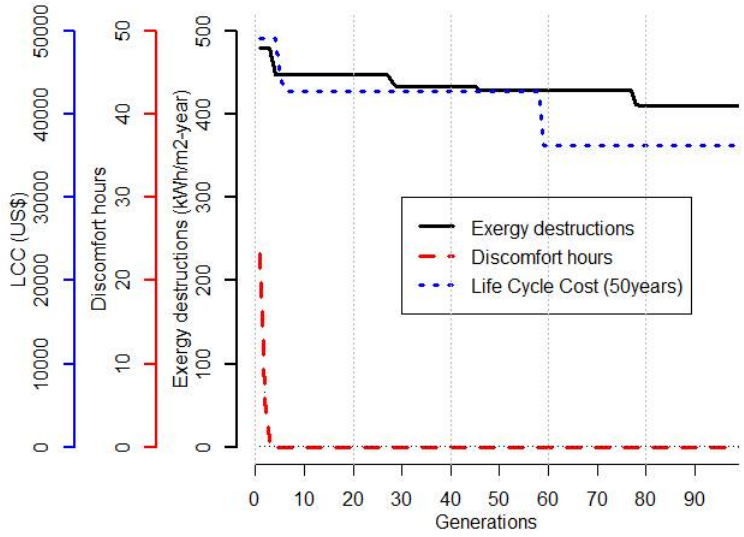

Figure 9: Convergence test of each objective function during the optimisation process

3.3. Compromise programming: the closest to utopia (CTU) design

As part of the tool's capabilities, a decision-making process has been implemented in order to choose a final optimal design that satisfies most of the objectives and to provide a comparative study with the baseline design. This would also locate those solutions that are weighting only one of the objectives exclusively, thus filtering those designs in the final consideration. From the Pareto front, and based on compromised programming, the Chebyshev distance (α_j) minimisation method has been applied to screen all possible solutions. In this case, weights for each objective are initialised and screened to obtain a series of compromised solutions. The method transforms a multi-objective problem into a single-objective one. The corresponding weight factors (p_j) reflect the relative importance of each objective, where the sum of weight coefficient has to satisfy the following constraint:

$$\sum_{j=1}^{n} p_j = 1 \tag{10}$$

Then, the Chebyshev distance can be calculated as follows:

$$\alpha_j \geq \left(\frac{|Z_j^* - Z_j(x)|}{|Z_j^* - Z_{*j}|} \right) * (p_j) \tag{11}$$

As the method scans all the feasible possible sets, it minimises the deviation from the ideal point, obtaining the minimum Chebyshev distance ([min]α_j [-]) and therefore a final design. This provides the decision maker with different trade-off scenarios. The whole screening of the Pareto front using the Chebyshev method can be found in the Supplementary Data (S.2). As shown, the multi-criteria method has been able to filter most of the solutions with high capital cost and moved on rather quickly from the right tail located in the Pareto front. This is illustrated as ASHPs appear in most of the compromised solutions instead of District Cooling, even though the latter is found four times the former in the Pareto front.

For further analysis, the equal weight or 'closest to utopia' (CTU) design, where p_{exergy}, $p_{discomfort}$, and p_{lcc} are all equal to 0.33, is selected. In Figure 8, the CTU design parameters have been highlighted. The CTU energy system schematic is represented in Figure 10, while the capital cost for energy-related measures is presented in Table 4. For this particular design, passive-related measures represent 54.2% of the design's capital cost.

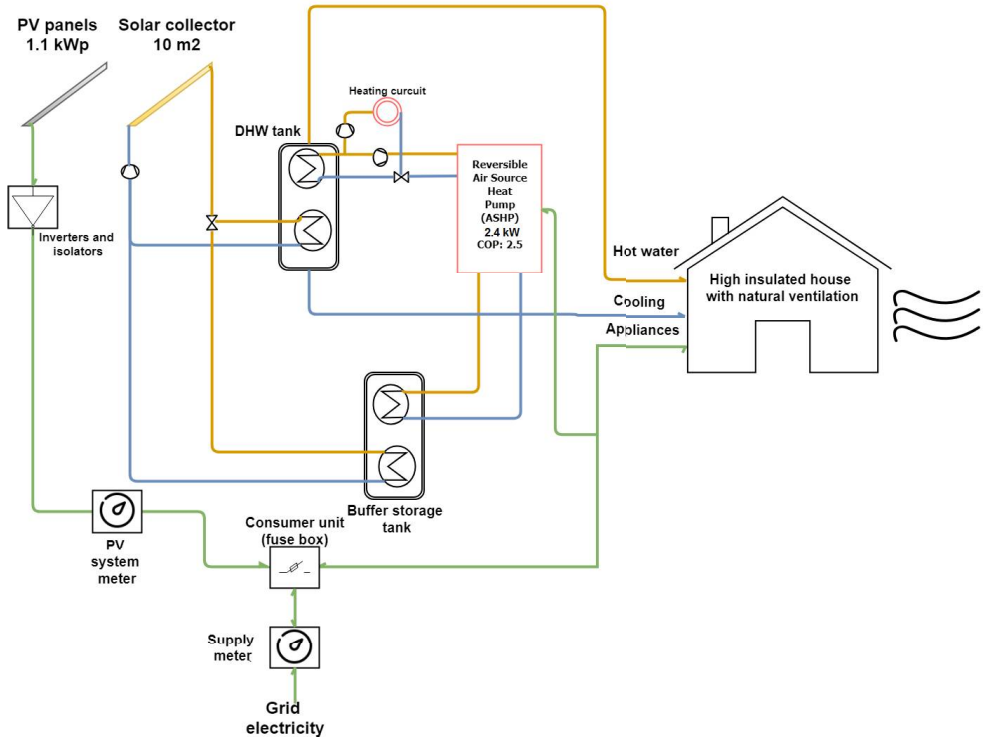

Figure 10: Closest to utopia (CTU) solution HVAC and energy system schematic

Table 4: Capital cost of energy related measures for the CTU solution [US$]

	CTU design technologies	Observations	Capital cost [US$]
Active systems	***Air source heat pump***	2.4 kW COP : 2.5 W/W	1,422
	HVAC distribution and emission system	insulated pipes, pumps and VAV systems	2,000
	Lighting	LED lighting (power: 3.7 W/m2)	144
	PV panels	1.1 kWp	5,794
	Solar collectors	10 m2	3,820
	Windows control	Actuators plus control system	2,000
Passive systems	***Glazing***	double-pane krypton filled	11,362
	Wall insulation	8.5 cm glass fibre	3,263
	Roof insulation	15 cm XPS	2,893
	Solar protection	**Front façade:** Overhangs 1.1 m Right fins: 0.15m Left fins: 1.55 m **Back façade:** Overhangs 0.2 m Right fins: 0.75m Left fins: 0.85 m **Left side façade:** Overhangs 1.2 m Right fins: 0.35m Left fins: 1.3 m	420
			33,118

Figure 11 presents the design day performance of the CTU design compared to the baseline. Wind directions (Figure 11a) and speeds (Figure 11b) for that specific day are illustrated. The evening peak demand (around 7 pm) has been greatly reduced due to optimal insulation levels and solar shading devices, as solar gains throughout the day were minimised which in turn reduced the amount of heat stored at the building's thermal mass. The entering cool sea breeze, especially in the morning (from 2 am to 5 am) and in the evening (from 8 pm to 11 pm), results in the reduction of internal temperatures. Overall, as natural ventilation rates have improved thermal comfort sensation, this has resulted in a reduction in hourly cooling demand as set-points were able to be increased on average 1.5 °C. Orientation and window control has resulted in internal average window velocities of 0.33 m s^{-1}.

The building cooling energy demand for that specific day has been reduced from 223 kWh day^{-1} to 154 kWh day^{-1}, while exergy demand has been reduced by two-thirds, from 50.4 kWh day^{-1} to 19.3 kWh day^{-1}, due to an optimal use and harvest of cool exergy from the thermal breezes. Finally, thanks to a more constant indoor thermal environment, this would make artificial cooling equipment work on a more regular basis, increasing its performance as it would not require to be constantly turned on and off. This also increases equipment's lifetime.

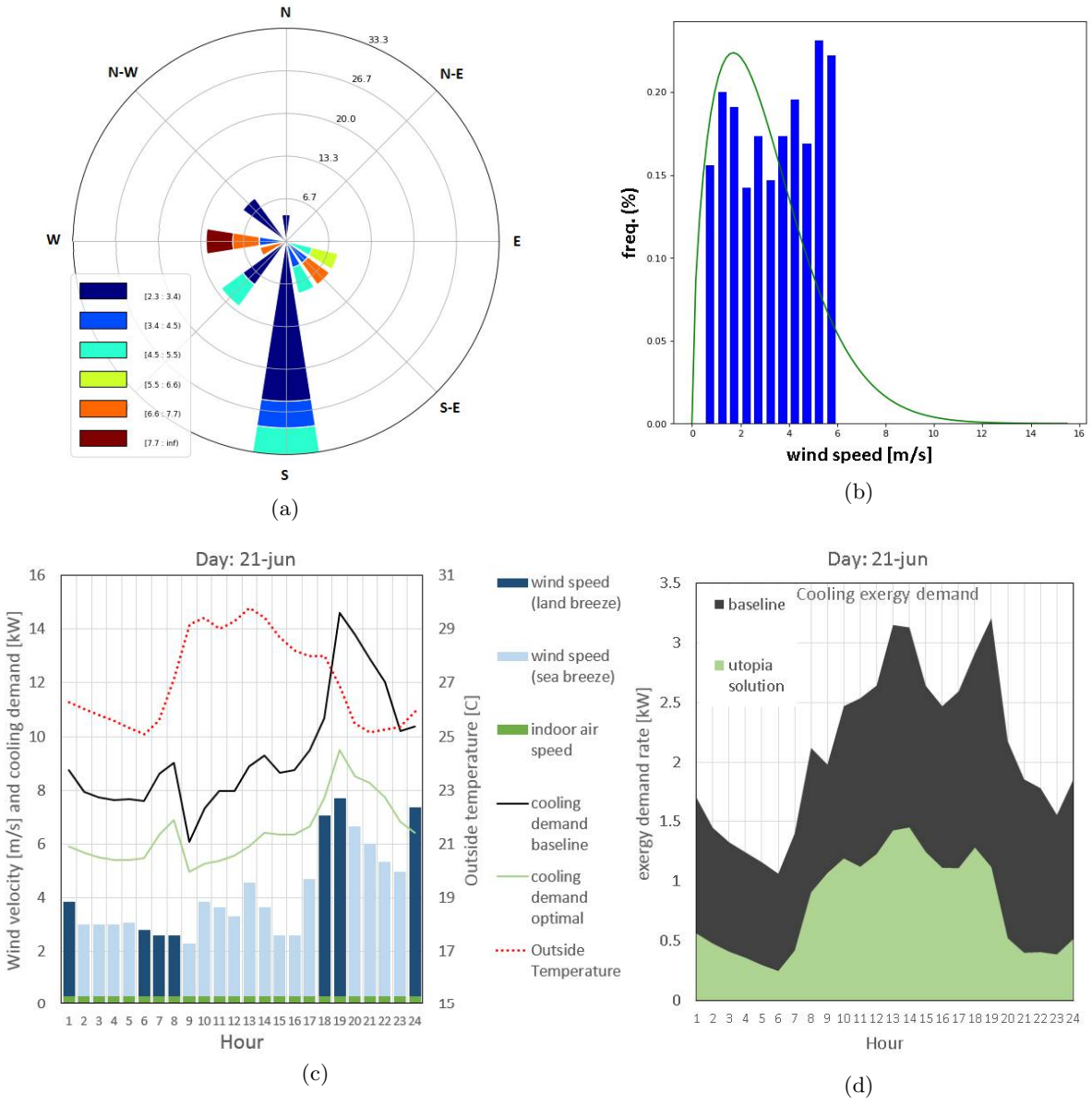

Figure 11: Design day climate data and energy/exergy demand comparison between the baseline and CTU design

Lastly, Table 5 presents the annual performance comparison considering the main studied indicators. Although gross energy demand has not been greatly reduced, if on-site generation is considered, the building reduced around half of its baseline grid demand. Although it can not be regarded as a low-exergy building due to still high exergy consumption rates, it has to be considered that almost one-third of the primary exergy input now comes from renewable sources (especially solar-based electricity and hot-water generation). As previously discussed, the orientation of the CTU design has been optimised to 30° relative to north, to make the best use of sunlight and natural ventilation from thermal breezes. This single bioclimatic low-cost measure contributes importantly to the reduction of energy demand and exergy consumption from the whole energy

supply chain while considerably improving occupant thermal comfort.

Although capital costs are higher than the baseline, reduced annual energy bills have resulted in an LCC increase of just 18.5% or US$ 7,381 over a 50 year period. This represents an annual increase in expenditure of about US$ 53 per household. If some level of incentives were to be considered due to on-site renewable generation, this could easily offset this cost increase. Certainly, the cost increase can be justified by the considerable improvement of indoor environmental conditions. This could have other non-energy benefits such as improved health conditions and lifestyle performance, implications that were not considered in this particular study.

Table 5: A comparison of main indicators between baseline and CTU design

Parameters	**Baseline**	**CTU Pareto**	**Difference (%)**
Primary energy (kWh m^2 y^{-1})	620.1	290.3	-53.2%
Site energy (kWh m^2 y^{-1})	278.1	250.2	-10.0%
PV electricity generation (kWh m^2 y^{-1})	0.0	13.9	n/a
Solar Thermal DHW generation (kWh m^2 y^{-1})	0.0	31.4	n/a
Net site energy (kWh m^2 y^{-1})	278.1	131.4	-52.7%
Primary exergy input (kWh m^2 y^{-1})	571.9	514.9	-10.0%
Exergy consumption (kWh m^2 y^{-1})	507.2	454.7	-10.3%
Building exergy efficiency	11.3%	11.7%	3.3%
Energy measures CAPEX (US$)	11,295.2	33,117.6	193.2%
Annual energy bill (US$)	2,210.4	1,098.6	-50.3%
Life Cycle Cost - 50 years (US$)	39,864.6	47,245.7	18.5%
Discomfort (hours)	1,459.7	89.8	-93.8%

3.4. Discussion

With the intention to make exergy-oriented optimisation more available for design practice, it is fundamental to provide robust methodological frameworks that produce cost-effective and comfortable designs under low-uncertainty levels. This study has combined exergy and bioclimatic analysis with optimisation and multi-criteria decision frameworks, yielding final solutions that satisfied thermodynamic and thermal comfort objectives with minimal increase in cost. Additionally, the presented optimisation framework, has been adapted to analyse the thermodynamic influence of the sea-land breeze effect. The research has demonstrated the necessity to consider the local environment at an early stage in the building design process. Exergy optimisation can be regarded as a more comprehensive method as it accounts for true thermodynamic efficiencies and locates exact sources of irreversibilities that should be minimised.

The low-exergy and bioclimatic approaches present some similarities, as most bioclimatic strategies can be regarded as exergy efficient, where the energy quality of supply sources are close to the demand quality of services (e.g. natural light for lighting demand or natural ventilation to cover cooling demands). However, technically, due to energy harvest limitations and real environmental dynamics, it is recommended that passive strategies are supported by active measures to achieve a desired thermal performance. This study has considered this limitation, as the tool aimed to first account for local low-exergy resources and then, if necessary, supplement the building system

with active measure with minimal thermodynamic losses. If the installation of artificial space conditioning is necessary, high-exergy efficient technologies should be encouraged (GSHP, low-exergy district cooling network); however, currently these come with considerable investments and operational costs. During the last decade, active solar technologies have experienced constant capital cost reduction resulting in higher uptake rates. A similar success could be expected for low-exergy technologies. An advantage of these technologies is that when in operation, they could provide an important reduction in primary energy demand as well as in operational cost while minimising the total environmental impact of the building and consequently the entire building stock. Nevertheless, cost-optimality of these measures will strongly depend on factors such as energy prices and government subsidies or incentives.

Although not part of this study, consideration of the urban design is also necessary. At a neighbourhood level, it is recommended for houses to be separated to optimise the breeze effect between buildings [14]. Poor urbanisation in the coast could limit the natural flow of sea-land breeze, leading to higher temperatures inland, negative health effects and large energy use by the intensification of cooling services. An increase in building standards that considers solar and wind resources in coastal areas, on both at building and urban levels, could support the development of a future decarbonised and more efficient housing stock.

4. Conclusions

Limited research has focused on optimising exergy and thermal comfort performance of coastal buildings located in tropical areas, where it is expected that artificial cooling will be responsible for a considerable share in future global electricity demand.

This study has included a wind energy/exergy analysis method that accounts for the thermodynamic performance of the thermal breeze in buildings. The model has been added into a multi-objective optimisation decision-support modelling tool capable of evaluating cost-efficient and low-exergy coastal housing designs with high thermal comfort performance. Additionally, specific active and passive strategies that aim at maximising the utilisation of local wind and solar resources have been developed. This approach supports building designers in complex decision making in coastal areas by considering the fundamental laws of thermodynamics.

The specific optimisation study has focused on performing a comprehensive exploration of a wide range state-of-the-art building energy technologies, with the intention to minimise energy use, improve thermodynamic performance as well as internal building thermal conditions with minimal life cycle cost increase. Overall, the main findings from this study confirmed the positive influence that the sea-land breeze effect could have when it is correctly adapted to the building design, as it improves the building's thermodynamic and thermal comfort performance. In the case study, wind and solar resources have been essential to improve most of the objective functions. On average, it was found that an optimal orientation, solar shading and ventilation flow control decreased thermal discomfort hours and increased thermal set-points of AC equipment by an average of 1.5°. On the other hand, solar collectors have been the most cost-effective solutions to cover hot water demand throughout the year. This could have significant carbon emissions and exergy consumption footprints reductions in the region by decreasing the demand of grid electricity, LPG and natural gas.

An equal weight design solution, where all objective functions were equally considered, reduced thermal discomfort to almost zero as well as one-tenth of total exergy consumption, whilst increasing life cycle cost by less than 20%. The main strength of a combined exergy and economic optimisation is the ability to thermodynamically and economically improve the design by reducing unnecessary irreversibilities in a cost-effective way. Other important objectives such as indoor air quality should be explored, especially for coastal housing located in the tropics where high indoor humidity can be expected. Poor humidity control could cause high levels of condensation, deteriorating indoor air quality and living standards.

For future work, other passive and active cooling strategies will be explored. Specifically, solar chimneys, trombe walls, desiccant cooling systems, intermittent absorptive solar-cooling systems, and absorption solar cooling are of interest. Furthermore, urban level optimisation would be conducted by applying the framework at a district level. Different levels of feed-in-tariffs and renewable generation incentives would be considered to find optimal values that could unlock low-energy designs with high exergy-efficiency. Finally, it is indented to include carbon and exergetic life cycle analysis to understand the impact of embodied carbon and exergy footprint on construction materials and equipment.

5. Acknowledgements

The first author would like to acknowledge the support of the 'Instituto de Ingenieria, UNAM' and 'CEMIE-Oceano' for funding this work.

Nomenclature

Abbreviations

$1P$	single-pane window
$2P$	double-pane window
$3P$	triple-pane window
$AGEL$	aerogel
$ASHP$	air source heat pump
$CellG$	cellular glass
CFL	compact fluorescent lamps
COP	coefficient of performance
$CorkB$	cork board
DHW	domestic hot water
EPS	expanded polystyrene
$GFibre$	glass fibre

$GSHP$	ground source heat pump
$HVAC$	heating, ventilation and air conditioning
HX	heat exchanger
IEQ	indoor environmental quality
LED	light emitting diode
$PHEN$	phenolic foam board
PMV	predicted mean vote index
PUR	polyurethane
PV	photovoltaic
$TARP$	thermal analysis research program
UHI	urban heat island
VAV	variable air volume
XPS	extruded polystyrene

Greek symbols

α	wind speed profile exponent [-]
α_j	Chebyshev distance [-]
Δ	differential
δ	wind speed profile boundary layer thickness [-]
η	energy efficiency [%]
ψ	exergy efficiency [%]
ρ	outdoor air density [kg m^{-3}]

Nomenclature

$\dot{m}$	mass flow rate [kg s^{-1}]
$A_{opening}$	opening area [m^2]
C_p	specific heat coefficient [1.007 kJ $kg^{-1}K^{-1}$]
$c_{p,heat}$	specific heat [J K^{-1}]
C_w	opening effectiveness [dimensionless]
En	energy [kWh]

Ex	exergy [kWh]
$F_{schedule}$	open area fraction [m]
G	incident solar radiation [W m^2]
g	gravitational acceleration [9.81 m s^{-2}]
LCC	life cycle cost [US$]
Q_w	volumetric air flow rate [m3 s^{-1}]
T_0	outdoor temperature [deg]
T_i	inside temperature [deg]
U_{value}	thermal transmittance [W m^{-2}]
V	wind speed at altitude z [m s^{-1}]
Z	objective function
C_en	annual energy cost [US$]
C_n	capital cost [US$]
CF_n	annual cash flow [US$ y^{-1}]
F_p	fuel primary energy factor [-]
F_q	fuel quality factor [-]
$O\&M_n$	operation and maintenance cost [US$]
r_d	discount rate [%]

Subscripts and superscripts

appl	appliances
arg	argon
col	solar collector
cons	consumption
cook	cooking
dem	demand
f	fuel type f
i	thermal zone i
krp	krypton

met	meteorological station
n	number of thermal zones
prim	primary energy
ref	refrigeration
vent	ventilation
z	height above ground of the wind speed sensor [m]

References

[1] C. Small, R. J. Nicholls, A Global Analysis of Human Settlement in Coastal Zones, Journal of Coastal Research 19 (3) (2003) 584–599, ISSN 07490208, 15515036, URL http://www.jstor.org/stable/4299200.

[2] IPCC, Fifth Assessment Report of the Intergovernmental Panel on Climate Change, Report, 2014.

[3] J. Iwaro, A. Mwasha, A review of building energy regulation and policy for energy conservation in developing countries, Energy Policy 38 (12) (2010) 7744 – 7755, ISSN 0301-4215, doi:https://doi.org/10.1016/j.enpol.2010.08.027, URL http://www.sciencedirect.com/science/article/pii/S0301421510006427, special Section: Carbon Reduction at Community Scale.

[4] E. D. L. Patino, J. A. Siegel, Indoor environmental quality in social housing: A literature review, Building and Environment 131 (2018) 231 – 241, ISSN 0360-1323, doi:https://doi.org/10.1016/j.buildenv.2018.01.013, URL http://www.sciencedirect.com/science/article/pii/S0360132318300192.

[5] M. Indraganti, K. D. Rao, Effect of age, gender, economic group and tenure on thermal comfort: A field study in residential buildings in hot and dry climate with seasonal variations, Energy and Buildings 42 (3) (2010) 273 – 281, ISSN 0378-7788, doi:https://doi.org/10.1016/j.enbuild.2009.09.003, URL http://www.sciencedirect.com/science/article/pii/S0378778809002175.

[6] S. Copiello, L. Gabrielli, Analysis of building energy consumption through panel data: The role played by the economic drivers, Energy and Buildings 145 (2017) 130 – 143, ISSN 0378-7788, doi:https://doi.org/10.1016/j.enbuild.2017.03.053, URL http://www.sciencedirect.com/science/article/pii/S0378778817301925.

[7] IEA, The Future of Cooling: Opportunities for energy-efficient air conditioning, Report, OECD/IEA, 2018.

[8] UN, Framework Convention on Climate Change: Adoption of the Paris Agreement, Report, United Nations, 2015.

[9] B. F. Giannetti, J. C. Demtrio, F. Agostinho, C. M. Almeida, G. Liu, Towards more sustainable social housing projects: Recognizing the importance of using local resources, Building and Environment 127 (2018) 187 – 203, ISSN 0360-1323, doi:https://doi.org/10.1016/j.buildenv.2017.10.033, URL http://www.sciencedirect.com/science/article/pii/S0360132317304912.

[10] A. McCabe, D. Pojani, A. B. van Groenou, The application of renewable energy to social housing: A systematic review, Energy Policy 114 (2018) 549 – 557, ISSN 0301-4215, doi:https://doi.org/10.1016/j.enpol.2017.12.031, URL http://www.sciencedirect.com/science/article/pii/S030142151730856X.

[11] G. Desogus, L. G. F. Cannas, A. Sanna, Bioclimatic lessons from Mediterranean vernacular architecture: The Sardinian case study, Energy and Buildings 129 (2016) 574 – 588, ISSN 0378-7788, doi:https://doi.org/10.1016/j.enbuild.2016.07.051, URL http://www.sciencedirect.com/science/article/pii/S0378778816306612.

[12] S. Mirrahimi, M. F. Mohamed, L. C. Haw, N. L. N. Ibrahim, W. F. M. Yusoff, A. Aflaki, The effect of building envelope on the thermal comfort and energy saving for high-rise buildings in hothumid climate, Renewable and Sustainable Energy Reviews 53 (2016) 1508 – 1519, ISSN 1364-0321, doi:https://doi.org/10.1016/j.rser.2015.09.055, URL http://www.sciencedirect.com/science/article/pii/S1364032115010254.

[13] B. Lebassi, J. E. Gonzlez, R. D. Bornstein, On the Environmental Sustainability of Building Integrated Solar Technologies in a Coastal City, Journal of Solar Energy Engineering 135 (4) (2013) 040904–040904–6, ISSN 0199-6231, doi:10.1115/1.4025507, URL http://dx.doi.org/10.1115/1.4025507, 10.1115/1.4025507.

[14] R. Shanthi Priya, M. C. Sundarraja, S. Radhakrishnan, L. Vijayalakshmi, Solar passive techniques in the vernacular buildings of coastal regions in Nagapattinam, TamilNadu-India a qualitative and quantitative analysis, Energy and Buildings 49 (2012) 50–61, ISSN 0378-7788, doi:https://doi.org/10.1016/j.enbuild.2011.09.033, URL http://www.sciencedirect.com/science/article/pii/S037877881100435X.

[15] A. Lavagnini, A. M. Sempreviva, R. J. Barthelmie, Estimating Wind Energy Potential Offshore in Mediterranean Areas, Wind Energy 6 (1) (2003) 23–34, doi:doi:10.1002/we.81, URL https://onlinelibrary.wiley.com/doi/abs/10.1002/we.81.

[16] C. J. Steele, S. R. Dorling, R. v. Glasow, J. Bacon, Modelling seabreeze climatologies and interactions on coasts in the southern North Sea: implications for offshore wind energy, Quarterly Journal of the Royal Meteorological Society 141 (690) (2015) 1821–1835, doi:doi:10.1002/qj.2484, URL https://rmets.onlinelibrary.wiley.com/doi/abs/10.1002/qj.2484.

[17] H. Chien, H. Cheng, K. Yang, Y. Tsai, W. Chang, Diurnal and semidiurnal variability of coastal wind over Taiwanese waters, Wind Energy 18 (8) (2015) 1353–1370, doi:doi:10.1002/we.1761, URL https://onlinelibrary.wiley.com/doi/abs/10.1002/we.1761.

[18] M. G. Hughes, A. D. Heap, National-scale wave energy resource assessment for Australia, Renewable Energy 35 (8) (2010) 1783–1791, ISSN 0960-1481, doi:https://doi.org/10.1016/j.renene.2009.11.001, URL http://www.sciencedirect.com/science/article/pii/S0960148109004777.

[19] C. V. Srinivas, R. Venkatesan, A. Bagavath Singh, Sensitivity of mesoscale simulations of land-sea breeze to boundary layer turbulence parameterization, Atmospheric Environment 41 (12) (2007) 2534–2548, ISSN 1352-2310, doi:https://doi.org/10.1016/j.atmosenv.2006.11.027, URL http://www.sciencedirect.com/science/article/pii/S1352231006011654.

[20] T. Tirabassi, F. Fortezza, W. Vandini, Wind circulation and air pollutant concentration in the coastal city of ravenna, Energy and Buildings 16 (1) (1991) 699–704, ISSN 0378-7788, doi:https://doi.org/10.1016/0378-7788(91)90040-A, URL http://www.sciencedirect.com/science/article/pii/037877889190040A.

[21] R. Pokhrel, H. Lee, Estimation of the effective zone of sea/land breeze in a coastal area, Atmospheric Pollution Research 2 (1) (2011) 106–115, ISSN 1309-1042, doi:https://doi.org/10.5094/APR.2011.013, URL http://www.sciencedirect.com/science/article/pii/S1309104215305225.

[22] Z. Liang, D. Wang, Sea breeze and precipitation over Hainan Island, Quarterly Journal of the Royal Meteorological Society 143 (702) (2017) 137–151, doi:doi:10.1002/qj.2952, URL https://rmets.onlinelibrary.wiley.com/doi/abs/10.1002/qj.2952.

[23] N. Pesic, J. R. Calzada, A. M. Alcojor, Natural ventilation potential of the Mediterranean coastal region of Catalonia, Energy and Buildings 169 (2018) 236 – 244, ISSN 0378-7788, doi:https://doi.org/10.1016/j.enbuild.2018.03.061, URL http://www.sciencedirect.com/science/article/pii/S0378778817340513.

[24] J.-I. Tsutsumi, T. Katayama, T. Hayashi, H. Kitayama, A. Ishii, Statistical analysis for the characteristics of sea-land breeze and its effect on urban thermal environment, Energy and Buildings 16 (3) (1991) 1003–1008, ISSN 0378-7788, doi:https://doi.org/10.1016/0378-7788(91)90095-K, URL http://www.sciencedirect.com/science/article/pii/037877889190095K.

[25] A. Salvati, H. Coch Roura, C. Cecere, Assessing the urban heat island and its energy impact on residential buildings in Mediterranean climate: Barcelona case study, Energy and Buildings 146 (2017) 38–54, ISSN 0378-7788, doi:https://doi.org/10.1016/j.enbuild.2017.04.025, URL http://www.sciencedirect.com/science/article/pii/S0378778817312914.

[26] E. D. Freitas, C. M. Rozoff, W. R. Cotton, P. L. S. Dias, Interactions of an urban heat island and sea-breeze circulations during winter over the metropolitan area of So Paulo, Brazil, Boundary-Layer Meteorology 122 (1) (2007) 43–65, ISSN 1573-1472, doi:10.1007/s10546-006-9091-3, URL https://doi.org/10.1007/s10546-006-9091-3.

[27] T. Ichinose, K. Shimodozono, K. Hanaki, Impact of anthropogenic heat on urban climate in Tokyo, Atmospheric Environment 33 (24) (1999) 3897–3909, ISSN 1352-2310, doi:https://doi.org/10.1016/S1352-2310(99)00132-6, URL http://www.sciencedirect.com/science/article/pii/S1352231099001326.

[28] W. J. Batty, H. Al-Hinai, S. D. Probert, Natural-cooling techniques for residential buildings in hot climates, Applied Energy 39 (4) (1991) 301–337, ISSN 0306-2619, doi:https://doi.org/10.1016/0306-2619(91)90002-F, URL http://www.sciencedirect.com/science/article/pii/030626199190002F.

[29] T. Katayama, T. Hayashi, Y. Shiotsuki, H. Kitayama, A. Ishii, M. Nishida, J.-I. Tsutsumi, M. Oguro, Cooling effects of a river and sea breeze on the thermal environment in a built-up area, Energy and Buildings 16 (3) (1991) 973–978, ISSN 0378-7788, doi:https://doi.org/10.1016/0378-7788(91)90092-H, URL http://www.sciencedirect.com/science/article/pii/037877889190092H.

[30] G. A. Faggianelli, A. Brun, E. Wurtz, M. Muselli, Assessment of different airflow mod-

eling approaches on a naturally ventilated Mediterranean building, Energy and Buildings 107 (2015) 345–354, ISSN 0378-7788, doi:https://doi.org/10.1016/j.enbuild.2015.08.038, URL http://www.sciencedirect.com/science/article/pii/S0378778815302206.

[31] A. Aflaki, N. Mahyuddin, Z. Al-Cheikh Mahmoud, M. R. Baharum, A review on natural ventilation applications through building faade components and ventilation openings in tropical climates, Energy and Buildings 101 (2015) 153–162, ISSN 0378-7788, doi:https://doi.org/10.1016/j.enbuild.2015.04.033, URL http://www.sciencedirect.com/science/article/pii/S0378778815003321.

[32] J. Xie, Y. Cui, J. Liu, J. Wang, H. Zhang, Study on convective heat transfer coefficient on vertical external surface of island-reef building based on naphthalene sublimation method, Energy and Buildings 158 (2018) 300–309, ISSN 0378-7788, doi:https://doi.org/10.1016/j.enbuild.2017.09.092, URL http://www.sciencedirect.com/science/article/pii/S0378778817315980.

[33] G. A. Faggianelli, A. Brun, E. Wurtz, M. Muselli, Natural cross ventilation in buildings on Mediterranean coastal zones, Energy and Buildings 77 (2014) 206–218, ISSN 0378-7788, doi:https://doi.org/10.1016/j.enbuild.2014.03.042, URL http://www.sciencedirect.com/science/article/pii/S037877881400262X.

[34] A. Rinaldi, M. Roccotelli, A. M. Mangini, M. P. Fanti, F. Iannone, Natural Ventilation for Passive Cooling by Means of Optimized Control Logics, Procedia Engineering 180 (2017) 841 – 850, ISSN 1877-7058, doi:https://doi.org/10.1016/j.proeng.2017.04.245, URL http://www.sciencedirect.com/science/article/pii/S1877705817317526, international High-Performance Built Environment Conference A Sustainable Built Environment Conference 2016 Series (SBE16), iHBE 2016.

[35] C. R. Bullen, A low energy housing design in an area of high wind and rain: An innovative housing scheme at Stenness on the Orkney islands, Energy and Buildings 32 (3) (2000) 319–326, ISSN 0378-7788, doi:https://doi.org/10.1016/S0378-7788(00)00059-1, URL http://www.sciencedirect.com/science/article/pii/S0378778800000591.

[36] B. Lebassi, J. E. Gonzlez, D. Fabris, R. Bornstein, Impacts of Climate Change in Degree Days and Energy Demand in Coastal California, Journal of Solar Energy Engineering 132 (3) (2010) 031005–031005–9, ISSN 0199-6231, doi:10.1115/1.4001564, URL http://dx.doi.org/10.1115/1.4001564, 10.1115/1.4001564.

[37] H. Radhi, S. Sharples, Quantifying the domestic electricity consumption for air-conditioning due to urban heat islands in hot arid regions, Applied Energy 112 (2013) 371–380, ISSN 0306-2619, doi:https://doi.org/10.1016/j.apenergy.2013.06.013, URL http://www.sciencedirect.com/science/article/pii/S0306261913005205.

[38] H. Mittal, A. Sharma, A. Gairola, A review on the study of urban wind at the pedestrian level around buildings, Journal of Building Engineering 18 (2018) 154 – 163, ISSN 2352-7102, doi:https://doi.org/10.1016/j.jobe.2018.03.006, URL http://www.sciencedirect.com/science/article/pii/S2352710217307581.

[39] P. Rajagopalan, K. C. Lim, E. Jamei, Urban heat island and wind flow characteristics of a tropical city, Solar Energy 107 (2014) 159–170, ISSN 0038-092X, doi:https://doi.org/10.1016/j.solener.2014.05.042, URL http://www.sciencedirect.com/science/article/pii/S0038092X14002825.

[40] J. Szargut, Potential balance in chemical processes (in Polish), Arch. Budowy Maszyn 4 (11) (1957) 89–117.

[41] M. A. Rosen, I. Dincer, Exergy as the confluence of energy, environment and sustainable development, Exergy, An International Journal 1 (1) (2001) 3–13, ISSN 1164-0235, doi:http://dx.doi.org/10.1016/S1164-0235(01)00004-8, URL http://www.sciencedirect.com/science/article/pii/S1164023501000048.

[42] I. Dincer, C. Zamfirescu, Sustainable Energy Systems and Applications, Springer, US, ISBN 78-0-387-95860-6, doi:10.1007/978-0-387-95861-3, 2012.

[43] A. Agazzani, A. F. Massardo, A Tool for Thermoeconomic Analysis and Optimization of Gas, Steam, and Combined Plants, Journal of Engineering for Gas Turbines and Power 119 (4) (1997) 885–892, ISSN 0742-4795, doi:10.1115/1.2817069, URL http://dx.doi.org/10.1115/1.2817069, 10.1115/1.2817069.

[44] I. García Kerdan, R. Raslan, P. Ruyssevelt, D. Morillón Gálvez, A comparison of an energy/economic-based against an exergoeconomic-based multi-objective optimisation for low carbon building energy design, Energy 128 (2017) 244 – 263, ISSN 0360-5442, doi:https://doi.org/10.1016/j.energy.2017.03.142, URL http://www.sciencedirect.com/science/article/pii/S0360544217305352.

[45] V. Verda, E. Guelpa, A. Kona, S. Lo Russo, Reduction of primary energy needs in urban areas trough optimal planning of district heating and heat pump installations, Energy 48 (1) (2012) 40–46, ISSN 0360-5442, doi:http://dx.doi.org/10.1016/j.energy.2012.07.001, URL http://www.sciencedirect.com/science/article/pii/S0360544212005312.

[46] A. Bagdanavicius, N. Jenkins, G. P. Hammond, Assessment of community energy

supply systems using energy, exergy and exergoeconomic analysis, Energy 45 (1) (2012) 247–255, ISSN 0360-5442, doi:http://dx.doi.org/10.1016/j.energy.2012.01.058, URL http://www.sciencedirect.com/science/article/pii/S0360544212000631.

[47] H. Li, S. Svendsen, Energy and exergy analysis of low temperature district heating network, Energy 45 (1) (2012) 237–246, ISSN 0360-5442, doi:http://dx.doi.org/10.1016/j.energy.2012.03.056, URL http://www.sciencedirect.com/science/article/pii/S0360544212002599.

[48] D. Favrat, F. Marechal, O. Epelly, The challenge of introducing an exergy indicator in a local law on energy, Energy 33 (2) (2008) 130–136, ISSN 0360-5442, doi:http://dx.doi.org/10.1016/j.energy.2007.10.012, URL http://www.sciencedirect.com/science/article/pii/S0360544207001892.

[49] I. García Kerdan, R. Raslan, P. Ruyssevelt, D. Morillón Gálvez, The role of an exergy-based building stock model for exploration of future decarbonisation scenarios and policy making, Energy Policy 105 (2017) 467 – 483, ISSN 0301-4215, doi:https://doi.org/10.1016/j.enpol.2017.03.020, URL http://www.sciencedirect.com/science/article/pii/S0301421517301647.

[50] M. Shukuya, Energy, Entropy, Exergy and Space Heating Systems, in: L. Bnhidi (Ed.), Healthy Buildings '94: proceedings of the 3rd international conference, Technical University of Budapest, 369–374, 1994.

[51] E. Nieuwlaar, D. Dijk, Exergy evaluation of space-heating options, Energy 18 (7) (1993) 779–790, ISSN 0360-5442, doi:http://dx.doi.org/10.1016/0360-5442(93)90036-D, URL http://www.sciencedirect.com/science/article/pii/036054429390036D.

[52] F. Meggers, V. Ritter, P. Goffin, M. Baetschmann, H. Leibundgut, Low exergy building systems implementation, Energy 41 (1) (2012) 48–55, ISSN 0360-5442, doi:http://dx.doi.org/10.1016/j.energy.2011.07.031, URL http://www.sciencedirect.com/science/article/pii/S0360544211004798.

[53] F. Meggers, J. Pantelic, L. Baldini, E. M. Saber, M. K. Kim, Evaluating and adapting low exergy systems with decentralized ventilation for tropical climates, Energy and Buildings 67 (0) (2013) 559–567, ISSN 0378-7788, doi:http://dx.doi.org/10.1016/j.enbuild.2013.08.015, URL http://www.sciencedirect.com/science/article/pii/S0378778813005124.

[54] M. Schweiker, M. Shukuya, Adaptive comfort from the viewpoint of human body exergy consumption, Building and Environment 51 (2012) 351 – 360, ISSN 0360-1323, doi:https://doi.org/10.1016/j.buildenv.2011.11.012, URL http://www.sciencedirect.com/science/article/pii/S0360132311003969.

[55] A. Hepbasli, Low exergy (LowEx) heating and cooling systems for sustainable buildings and societies, Renewable and Sustainable Energy Reviews 16 (1) (2012) 73–104, ISSN 1364-0321, doi:http://dx.doi.org/10.1016/j.rser.2011.07.138, URL http://www.sciencedirect.com/science/article/pii/S1364032111003856.

[56] I. García Kerdan, R. Raslan, P. Ruyssevelt, S. Vaiciulyte, D. Morillón Gálvez, Thermodynamic and exergoeconomic analysis of a non-domestic Passivhaus retrofit, Building and Environment 117 (2017) 100 – 117, ISSN 0360-1323, doi:https://doi.org/10.1016/j.buildenv.2017.03.003, URL http://www.sciencedirect.com/science/article/pii/S0360132317300896.

[57] ECB-Annex49, Detailed Exergy Assessment Guidebook for the Built Environment, IEA ECBCS, Report, Fraunhofer IBP, 2011.

[58] A. Angelotti, P. Caputo, G. Solani, Dynamic exergy analysis of an air source heat pump, 1st International Exergy, Life Cycle Assessment, and Sustainability Workshop & Symposium (ELCAS) (2009) 8.

[59] W. Choi, R. Ooka, M. Shukuya, Exergy analysis for unsteady-state heat conduction, International Journal of Heat and Mass Transfer 116 (2018) 1124 – 1142, ISSN 0017-9310, doi:https://doi.org/10.1016/j.ijheatmasstransfer.2017.09.057, URL http://www.sciencedirect.com/science/article/pii/S0017931017320185.

[60] M. Pons, On the Reference State for Exergy when Ambient Temperature Fluctuates, International Journal of Thermodynamics 12 (3) (2009) 113–121, ISSN 1301-9724.

[61] R. Li, R. Ooka, M. Shukuya, Theoretical analysis on ground source heat pump and air source heat pump systems by the concepts of cool and warm exergy, Energy and Buildings 75 (2014) 447 – 455, ISSN 0378-7788, doi:https://doi.org/10.1016/j.enbuild.2014.02.019, URL http://www.sciencedirect.com/science/article/pii/S0378778814001303.

[62] O. B. Kazanci, M. Shukuya, B. W. Olesen, Theoretical analysis of the performance of different cooling strategies with the concept of cool exergy, Building and Environment 100 (2016) 102 – 113, ISSN 0360-1323, doi:https://doi.org/10.1016/j.buildenv.2016.02.013, URL http://www.sciencedirect.com/science/article/pii/S0360132316300506.

[63] R. Evins, A review of computational optimisation methods applied to sustainable building design, Renewable and Sustainable Energy Reviews 22 (0) (2013)

230–245, ISSN 1364-0321, doi:http://dx.doi.org/10.1016/j.rser.2013.02.004, URL http://www.sciencedirect.com/science/article/pii/S1364032113000920.

[64] S. Attia, M. Hamdy, W. OBrien, S. Carlucci, Assessing gaps and needs for integrating building performance optimization tools in net zero energy buildings design, Energy and Buildings 60 (0) (2013) 110–124, ISSN 0378-7788, doi:http://dx.doi.org/10.1016/j.enbuild.2013.01.016, URL http://www.sciencedirect.com/science/article/pii/S0378778813000339.

[65] F. Ascione, N. Bianco, C. De Stasio, G. M. Mauro, G. P. Vanoli, Artificial neural networks to predict energy performance and retrofit scenarios for any member of a building category: A novel approach, Energy 118 (2017) 999–1017, ISSN 0360-5442, doi:https://doi.org/10.1016/j.energy.2016.10.126, URL http://www.sciencedirect.com/science/article/pii/S0360544216315729.

[66] R. Wu, G. Mavromatidis, K. Orehounig, J. Carmeliet, Multiobjective optimisation of energy systems and building envelope retrofit in a residential community, Applied Energy 190 (2017) 634–649, ISSN 0306-2619, doi:https://doi.org/10.1016/j.apenergy.2016.12.161, URL http://www.sciencedirect.com/science/article/pii/S0306261916319419.

[67] S. Miglani, K. Orehounig, J. Carmeliet, Integrating a thermal model of ground source heat pumps and solar regeneration within building energy system optimization, Applied Energy 218 (2018) 78–94, ISSN 0306-2619, doi:https://doi.org/10.1016/j.apenergy.2018.02.173, URL http://www.sciencedirect.com/science/article/pii/S0306261918303076.

[68] Y. Fan, X. Xia, A multi-objective optimization model for energy-efficiency building envelope retrofitting plan with rooftop PV system installation and maintenance, Applied Energy 189 (2017) 327–335, ISSN 0306-2619, doi:https://doi.org/10.1016/j.apenergy.2016.12.077, URL http://www.sciencedirect.com/science/article/pii/S0306261916318505.

[69] A. Mariaud, S. Acha, N. Ekins-Daukes, N. Shah, C. N. Markides, Integrated optimisation of photovoltaic and battery storage systems for UK commercial buildings, Applied Energy 199 (2017) 466–478, ISSN 0306-2619, doi:https://doi.org/10.1016/j.apenergy.2017.04.067, URL http://www.sciencedirect.com/science/article/pii/S0306261917304646.

[70] Y. Cascone, A. Capozzoli, M. Perino, Optimisation analysis of PCM-enhanced opaque building envelope components for the energy retrofitting of office buildings in Mediterranean climates, Applied Energy 211 (2018) 929–953, ISSN 0306-2619, doi:https://doi.org/10.1016/j.apenergy.2017.11.081, URL http://www.sciencedirect.com/science/article/pii/S030626191731680X.

[71] X. Chen, H. Yang, Integrated energy performance optimization of a passively designed high-rise residential building in different climatic zones of China, Applied Energy 215 (2018) 145–158, ISSN 0306-2619, doi:https://doi.org/10.1016/j.apenergy.2018.01.099, URL http://www.sciencedirect.com/science/article/pii/S0306261918301132.

[72] I. García Kerdan, R. Raslan, P. Ruyssevelt, An exergy-based multi-objective optimisation model for energy retrofit strategies in non-domestic buildings, Energy 117, Part 2 (2016) 506–522, ISSN 0360-5442, doi:http://dx.doi.org/10.1016/j.energy.2016.06.041, URL http://www.sciencedirect.com/science/article/pii/S0360544216308155.

[73] I. García Kerdan, R. Raslan, P. Ruyssevelt, D. Morillón Gálvez, ExRET-Opt: An automated exergy/exergoeconomic simulation framework for building energy retrofit analysis and design optimisation, Applied Energy 192 (2017) 33–58, ISSN 0306-2619, doi:https://doi.org/10.1016/j.apenergy.2017.02.006, URL http://www.sciencedirect.com/science/article/pii/S0306261917301204.

[74] M. Di Somma, B. Yan, N. Bianco, G. Graditi, P. B. Luh, L. Mongibello, V. Naso, Multi-objective design optimization of distributed energy systems through cost and exergy assessments, Applied Energy 204 (2017) 1299–1316, ISSN 0306-2619, doi:https://doi.org/10.1016/j.apenergy.2017.03.105, URL http://www.sciencedirect.com/science/article/pii/S0306261917303483.

[75] EnergyPlus, EnergyPlus Engineering Reference, Report, 2012.

[76] Python-Software-Foundation, Python Language Reference version 2.7, URL http://www.python.org, 2018.

[77] A. Lazzaretto, G. Tsatsaronis, SPECO: A systematic and general methodology for calculating efficiencies and costs in thermal systems, Energy 31 (89) (2006) 1257–1289, ISSN 0360-5442, doi:http://dx.doi.org/10.1016/j.energy.2005.03.011, URL http://www.sciencedirect.com/science/article/pii/S0360544205000630.

[78] I. García Kerdan, R. Raslan, P. Ruyssevelt, D. Morillón Gálvez, An exergoeconomic-based parametric study to examine the effects of active and passive energy retrofit strategies for buildings, Energy and Buildings 133 (2016) 155–171, ISSN 0378-7788, doi:http://dx.doi.org/10.1016/j.enbuild.2016.09.029, URL http://www.sciencedirect.com/science/article/pii/S0378778816308404.

[79] ASHRAE, ASHRAE HandbookFundamentals Chapter 16, Ventilation and Infiltration, 2017.
[80] M. Shukuya, Exergy. Theory and Applications in the Built Environment, Green Energy and Technology, Springer London, ISBN 978-1-4471-4573-8, URL https://www.springer.com/gb/book/9781447145721, 2013.
[81] SENER, Balance Nacional de Energía 2016, URL https://www.gob.mx/sener/documentos/balance-nacional-de-energia, 2017.
[82] INECC, Inventario Nacional de Emisiones de Gases y Compuestos de Efecto Invernadero 2015, 2018.
[83] B. Faber, C. Gaubert, Tourism and Economic Development: Evidence from Mexico's Coastline, Working Paper 22300, National Bureau of Economic Research, doi:10.3386/w22300, URL http://www.nber.org/papers/w22300, 2016.
[84] I. Azuz-Adeath, E. Rivera-Arriaga, Descripción de la dinámica poblacional en la zona costera mexicana durante el periodo 2000-2005, Papeles de poblaciión 15 (2009) 75 – 107, ISSN 1405-7425.
[85] M. McNeil, S. Castellanos, D. Ponce De Leon Barido, P. Sánchez Pérez, Mexico space cooling electricity impacts and mitigation strategies: Analysis Supporting the Summit on Space Cooling Research Needs and Opportunities in Mexico, Report, 2018.
[86] SENER, Caracterizacin del uso de aire acondicionado en vivienda de inters social en Mxico (Characterization of air conditioners in low-income housing in Mexico), Report, 2018.
[87] CONUEE, Assessing energy savings from "Cool Roofs" on residential and non-residential buildings in Mexico, 2014.
[88] Meteonorm, Meteonorm: Irradiation data for every place on Earth, URL http://www.meteonorm.com/en/downloads, 2018.
[89] M. B. Maps, Cabo San Lucas, Baja California Sur, Mexico. Map, URL https://www.bing.com/maps, 2018.
[90] J. Lucero-Álvarez, N. A. Rodríguez-Munoz, I. R. Martín-Domínguez, The Effects of Roof and Wall Insulation on the Energy Costs of Low Income Housing in Mexico, Sustainability 8 (7), ISSN 2071-1050, doi:10.3390/su8070590, URL http://www.mdpi.com/2071-1050/8/7/590.
[91] D. Almada, F. Yeomans, C. Nungaray Perez, V. Hernandez Cordova, Monitoreo de Viviendas con Criterios de Ahorro Energético, in: LACCEI (Ed.), Ninth Latin American and Caribbean Conference (LACCEI2011), Engineering for a Smart Planet, Innovation, Information Technology and Computational Tools for Sustainable Development, August 3-5, Medellín, Colombia, 2011.
[92] ASHRAE, ASHRAE Guideline 14-2002: Measurement of Energy Demand and Savings, 2002.
[93] SENER, NOM-020-ENER-2011, 2011.
[94] Z. Utlu, A. Hepbasli, A study on the evaluation of energy utilization efficiency in the Turkish residential-commercial sector using energy and exergy analyses, Energy and Buildings 35 (11) (2003) 1145 – 1153, ISSN 0378-7788, doi:https://doi.org/10.1016/j.enbuild.2003.09.003, URL http://www.sciencedirect.com/science/article/pii/S0378778803001014.
[95] ASHRAE, ANSI/ASHRAE Standard 55-2004. Thermal Environmental Conditions for Human Occupancy, 2004.
[96] B. Givoni, Man, Climate and Architecture, Architectural Science Series, Applied Science Publ., URL https://books.google.co.uk/books?id=3E-0AAAAIAAJ, 1976.
[97] D. Schmidt, Methodology for the Modelling of Thermally Activated Building Components in Low Exergy Design, Phd thesis, 2004.
[98] H. Torio, Comparison and optimization of building energy supply systems through exergy analysis and its perspectives, Thesis, 2012.
[99] H. Torio, A. Angelotti, D. Schmidt, Exergy analysis of renewable energy-based climatisation systems for buildings: A critical view, Energy and Buildings 41 (3) (2009) 248–271, ISSN 0378-7788, doi:http://dx.doi.org/10.1016/j.enbuild.2008.10.006, URL http://www.sciencedirect.com/science/article/pii/S0378778808002211.

Appendix A: Exergy analysis within ExRET-Opt

The building thermal exergy method used in ExRET-Opt is mainly based on the developments proposed by Schmidt [97] and Torio [98]. Originally, the method used an input-output approach based on seven different subsystems (only thermal systems) to calculate exergy consumption throughout the energy supply chain. In addition, EXRET-Opt is also capable of calculating exergy use throughout the DHW system level, refrigeration, cooking, and all electric-based equipment, thus allowing for a holistic exergy assessment. This holistic method provides comprehensive

means by which to understand the interactions between the building envelope and the building energy services. Figure A.1 presents the 11 subsystems and 13 exergy flows analysed in the tool.

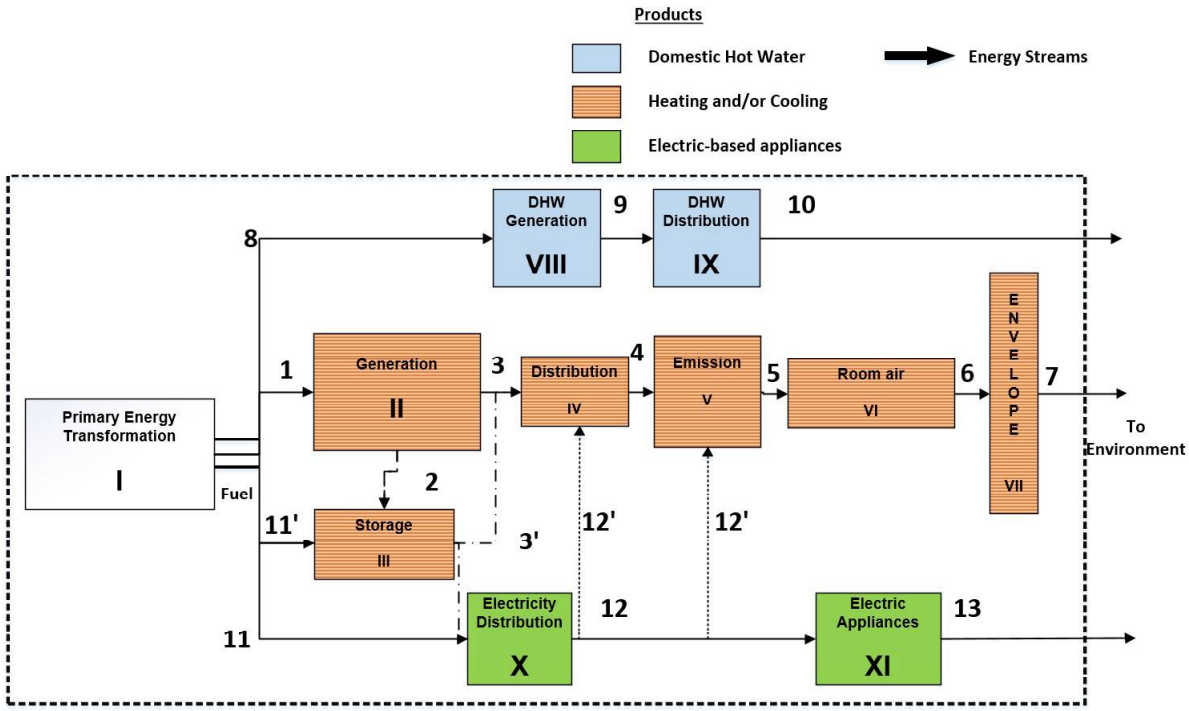

Figure A.1: Energy supply chain and subsystems for exergy calculations. Based on the IEA ECB Annex 49 method calculation.

The basic formulas for guidance are presented in the following section; however, a complete assessment of exergy analysis covering all the end-use services can be found in García Kerdan et al. [73].

A.1. Building exergy analysis

A.1.1. Exergy demand

The total exergy demand at the building level $\mathrm{Ex}_{dem,bui}$ is obtained by adding all the demands for each end-use (VI.cooling and heating, IX. domestic hot water, and XI. appliances):

$$Ex_{dem,bui}(t_k) = \sum_{i=1}^{i} Ex_{dem,enduse,i(t_k)} \tag{A.1}$$

where $Ex_{dem,enduse}$ is the exergy demand by end-use i.

Exergy demand for cooling purposes considering the effect of natural ventilation is calculated as showed in equation 3. For the rest of end use services, exergy demand is calculated as follows:

-Domestic hot water:

$$Ex_{dem,DHW}(t_k) = En_{DHW}(t_k) * \frac{\eta_{DHW}(t_k)}{F_q} * \left(1 - \frac{T_0(t_k)}{T_{HW}(t_k) - T_0(t_k)} ln \frac{T_{HW}(t_k)}{T_0(t_k)}\right) \quad \text{(A.2)}$$

where En_{DHW} is the domestic hot water energy demand, η_{DHW} is the DHW equipment efficiency, q_{fuel} is the quality factor of the energy source used, and T_{HW} is the hot water temperature.

-Cooking:

$$Ex_{dem,cook}(t_k) = En_{cook}(t_k) * \frac{\eta_{cook}(t_k)}{q_{fuel}} * \left(1 - \frac{T_0(t_k)}{T_{cook}(t_k)}\right) \quad \text{(A.3)}$$

where $En_{cook}(t_k)$ is the cooking energy demand, η_{cook} is the cooking equipment efficiency, and $T_{cook}(t_k)$ is the cooking temperature. Depending on the energy source (electricity, LPG or natural gas), q_{fuel} might vary.

-Refrigeration:

$$Ex_{dem,ref}(t_k) = En_{ref}(t_k) * COP_{ref}(t_k) * \left(\frac{T_0(t_k)}{T_{ref}(t_k)} - 1\right) \quad \text{(A.4)}$$

where En_{ref} is the energy demand for refrigeration, COP_{ref} is the refrigerators coefficient of performance, and T_{refr} is the refrigerators working temperature.

-Appliances
Most electric-based equipment is considered to have the same exergy and energy efficiency values.

$$Ex_{dem,el_{appl}}(t_k) = En_{dem,el_{appl}}(t_k) * F_{q,el} \quad \text{(A.5)}$$

where $En_{dem,el_appl}(t_k)$ is the energy demand for the electric-based equipment, and $F_{q,elec}$ is the quality factor of electricity (Table A.1).

A.1.2. Primary exergy analysis

After calculating total exergy demand, the model calculates exergy consumption at each subsystem level until reaching the start of the supply chain (I. Primary Energy Transformation). Exergy equations at subsystem level can be found elsewhere ([57], [73])

For primary exergy (Ex_{prim}) at the primary energy transformation (subsystem I. in Figure A.1) is calculated as follows:

$$Ex_{prim}(t_k) = \sum_{i=1}^{i} \left[\frac{En_{gen,i}(t_k)}{\eta_{gen,i}(t_k)} * F_{p,sources,i} * F_{q,sources,}\right] + \left[Ex_{dem,el_{appl}} * F_{p,elec}\right] \quad \text{(A.6)}$$

where, En_{gen} is the energy source used by the building HVAC, DHW, cooking or refrigeration system, η_{gen} is the system efficiency, $F_{p,source}$ is the fuel primary energy factor and $F_{q,source}$ is the fuel quality factor (Table 2).

Table A.1: Primary Energy Factors and Quality Factors by energy sources [36,45]

Energy source	**Primary energy factor [kWh/kWh]**	**Quality factor [kWh_{ex}/kWh_{en}]**
Natural gas	1.11	0.94
Electricity (Grid supplied)	2.58	1
District Energy	1.11	0.94
Oil	1.07	1
Biomass (Wood pellets)	1.2	1.05

If primary exergy comes from renewable sources and equipment this require a different exergy analysis from conventional systems as demonstrated by Torio et al. [99] While PV panels are regarded to have the same exergetic efficiency as its first law counterpart, for solar collectors is necessary a special assessment. To calculate the exergy of the incoming solar radiation to the equipment the following formula is used:

$$Ex_{sun}(t_k) = G(t_k) * A_{col} * \left(1 - \frac{T_0(t_k)}{T_{sun}(t_k)}\right) \tag{A.7}$$

where G is the incident solar radiation, A_{col} is the collector surface area, T_0 is the reference environment, and T_{sun} is the suns temperature, which is considered around 6000 K. This can be regarded as the first exergy input for the energy supply chain. Later, the output of the collector can be calculated as follows:

$$Ex_{col}(t_k) = \dot{m}(t_k) * c_{p,heat} * \left[\left(T_{out}(t_k) - T_{in}(t_k) - T_0(t_k) * ln\frac{T_{out}(t_k)}{T_{in}(t_k)}\right)\right] \tag{A.8}$$

where $\dot{m}(t_k)$ is the mass flow rate [kg s^{-1}], $c_{p,heat}$ is the carrier specific heat [J K^{-1}], T_{out} is the temperature provided by the collector, and T_in the return temperature to the collector. Finally, the exergy efficiency for solar collectors is obtained as follows:

$$\psi_{col}(t_k) = \frac{Ex_{col}(t_k)}{Ex_{sun}(t_k)} \tag{A.9}$$

Finally, to calculate the total exergy consumed in the building supply chain, the following equation is used:

$$Ex_{cons,bui}(t_k) = Ex_{prim}(t_k) - Ex_{dem,bui}(t_k) \tag{A.10}$$

Appendix B: NSGA-II optimisation process

ExRET-Opt approaches multi-objective optimisation by using a Non-Dominated Sorting Genetic Algorithm (NSGA-II), based on Charles Darwin's theory on evolution. Each of the building designs (or chromosomes) are composed of a set of design parameters (or genes). The selection of specific designs is undertaken through the 'survival of the fittest' principle, highlighting those that are closer to the desired objective(s). The most frequent design parameters located in the best designs often go through to the next generation, where new building designs with some (not all) characteristics have a better chance to be modelled. To avoid convergence into similar design parameters, the model simulates variability and recombination processes as some 'good' solutions

might have been lost in previous generations. Figure B.1 illustrates this process and the related software used in ExRET-Opt.

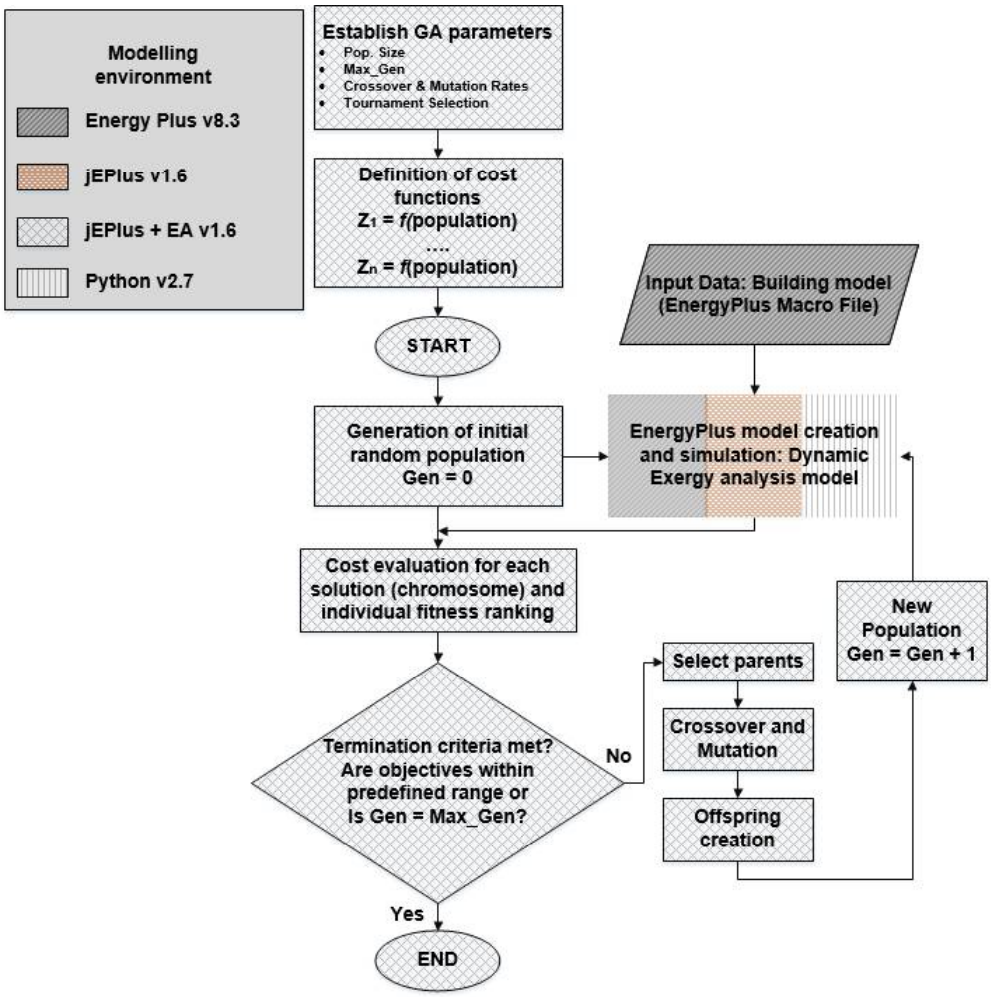

Figure B.1: Genetic algorithm optimisation process applied in ExRET-Opt[73]

Appendix C: Distributions of solar shading devices

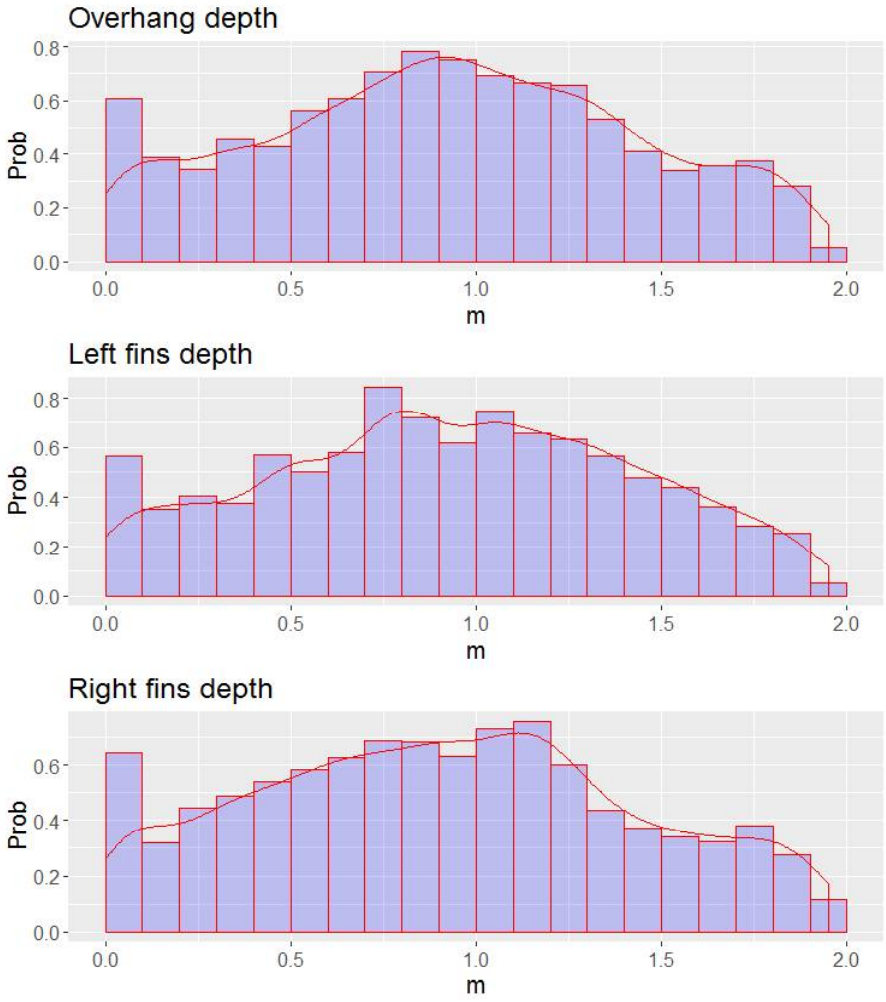

Figure C.1: Distribution (bars) and the fitted probability distribution (lines) of solar shading for the constrained solutions